Chapter 5. Differential Scanning Calorimetry

5.1 Introduction

The discussion in Chapter 2 clearly illustrates the fact that the crystallization process and the resulting morphology in polymers are largely governed by kinetic, more than thermodynamic factors. It is now clear that chain-folded lamellar crystals are associated with the crystallization of homopolymers under quiescent conditions. However, the presence of defects, such as branches along the polymer backbone imposes constraints on the chain-folding process. An increase in the overall concentration of branch points leads to a shift in the crystallizable sequence distribution to lower values and a decrease in the fraction of sequences which can participate in the chain-folded lamellar growth process at a given temperature. This leads to an increased proportion of non-crystallized chains in the amorphous regions between lamellae and thereby to a lower degree of crystallinity. The lamellae formed from branched chains are also characterized by a decrease in lateral dimensions when compared to those formed from their linear counterpart (as is confirmed through Atomic Force Microscopy in Chapter 6). The thermal analysis experiments described in this chapter are designed to understand the crystallization behavior of the sequences present in the amorphous regions, subsequent to initiation of the primary crystallization process in the ethylene/α-olefin copolymers. The results are correlated with characterization of the morphology subsequent to the crystallization process, and may also be related to the temporal evolution of other properties of the materials.

The experiments are designed to examine the effect of crystallization temperature, crystallization time, branch type and concentration on the nature of the melting and crystallization processes. The results of those experiments are presented in the Results section. This is followed by the Discussion section wherein the observed results are combined together to yield a preliminary model for the crystallization mechanism in the ethylene/α-olefin copolymers. Further studies to confirm the validity of the ideas proposed here will be presented in the following chapters.

5.2 Copolymer Sequence Distribution

It has been demonstrated previously[1,2,3,4,5] that the melting temperature and degree of crystallinity of a series of copolymers are, as a first approximation, independent of the nature of the comonomer (except for methyl branches), while being largely determined by the crystallizable sequence length distributions. It was alluded to in Chapter 2 that the sequence distributions are influenced by the type of catalyst (e.g., Ziegler-Natta based systems result in broader distributions compared to metallocene-based copolymers) used in the synthesis of the copolymers. It is important to address this aspect of the copolymers before proceeding to the details of the calorimetric experiments.

It was already established in Chapter 4 (by means of NMR studies) that the ethylene/α-olefin copolymers used in the present study conform to the random statistics for copolymers. This observation is further verified by the plots of weight percent crystallinities (the details of the determination of crystallinity data are given in the following section) and peak melting temperatures as functions of comonomer content, shown in Figure 1 and Figure 2 respectively. Figure 1 indicates that the crystallinities of all three types of copolymers can be represented by a single curve, irrespective of the comonomer type present. Due to differences in the size of the three types of comonomers compared, the percent of a comonomer required to yield a copolymer of given density is significantly different for the three comonomer types. As a result, the crystallinities derived for copolymers with a given mole percent comonomer, are identical to each other only when they are normalized with respect to the weight percent of crystallizable ethylene sequences available in the copolymer. Furthermore, the crystallinities of hydrogenated polybutadienes (HPBs) obtained from the literature[6,7] are also found to fall on the same curve. The HPBs are considered as model ethylene/1-butene random copolymers, whose compositional homogeneity is assured by the synthetic methods adopted,[8,9,10] and is known to be accurately determined. It follows that the copolymers examined conform to the random statistics expected of materials synthesized using the single-site constrained geometry catalyst technology. In addition, the fact that all three types of copolymers display an identical crystallinity behavior, in spite of their significantly different branch types - namely ethyl, propyl and butyl - implies that these

branches are predominantly excluded from the crystal lattice. This result is in accordance with the assumption of comonomer exclusion made in Flory's crystallization theory for copolymers.[11,12,13,14] Exclusion of the branch types mentioned above has also been established in a number of previous investigations.[15,16,17] The random statistics of the copolymers are further exemplified in Figure 2, where the melting temperatures of the copolymers as well as those of the HPBs are shown to be represented by a single curve.

5.3 Effect of Cooling Rate on the Crystallization Process

The crystallization behaviors of the ethylene/1-butene, ethylene/1-pentene and ethylene/1-hexene copolymers on cooling from the melt (180°C) to -20°C (using a dry ice/isopropanol mixture) at different cooling rates were examined. The rates studied ranged from 5 to 20°C/min. The corrected heat capacities estimated for the sample, EB-912, at two different cooling rates (5 and 20°C/min.) are shown in Figure 3. It has been previously demonstrated[4,18,19] that the crystallization process in such copolymers occurs over a broad temperature range, with significant increases in crystallinity even at temperatures as low as -20°C. In agreement with those observations, Figure 3 illustrates the presence of two distinct exotherms in the crystallization curves of the copolymer - a sharp exotherm at high temperatures and a much broader exotherm extending to very low temperatures. The temperature corresponding to the peak of the sharp crystallization exotherm is seen to be strongly rate-dependent, shifting to lower temperatures at higher cooling rates.

A major consideration in the estimation of heat capacities and degrees of crystallinity from the areas of crystallization exotherms is the accuracy of the baseline used in the calculation of peak areas. Incorrectly determined baselines can lead to significant errors in the crystallinity values. This concern is particularly significant in the case of copolymers, in view of the broad crystallization ranges involved. In order to verify the accuracy of the heat capacity calculations, the experimental values were compared to the $C_p(T)$ data for linear polyethylene reported by Wunderlich[20] (the solid line in Figure 3). It is reassuring to note that the experimental data in the melt display excellent agreement with the C_p values of linear PE in the melt. This result is also

consistent with previous reports in the literature,[4,20] indicating that the C_p^{melt} of the ethylene/α-olefin copolymers with branch concentrations less than ~15 mole %, are coincident with those for LPE.

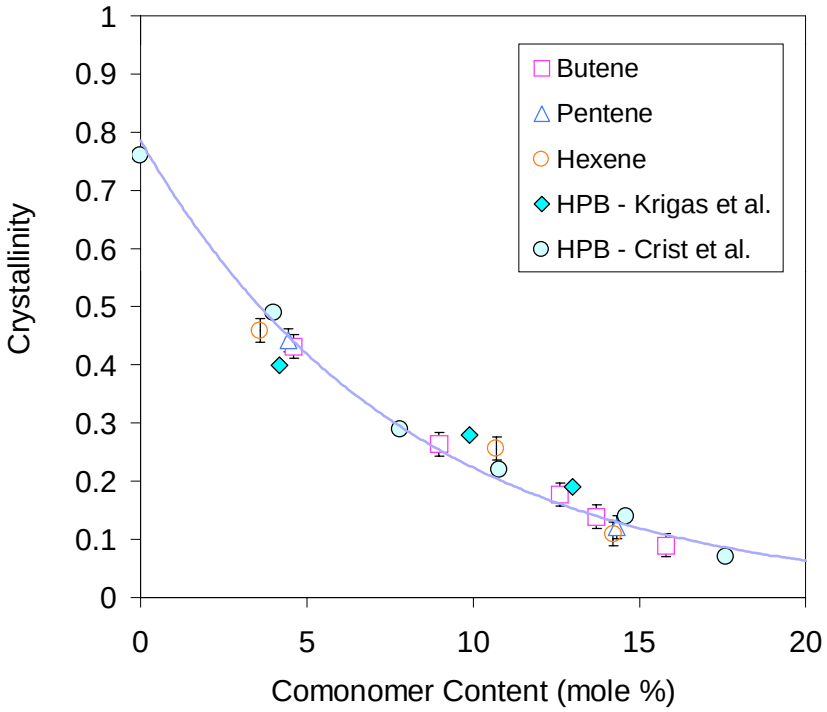

Figure 1 Degrees of crystallinity at -20°C for ethylene/1-butene, ethylene/1-pentene and ethylene/1-hexene copolymers (after cooling from the melt at 5°C/min) as a function of comonomer content. The crystallinity data for HPBs[6,7] are also included.

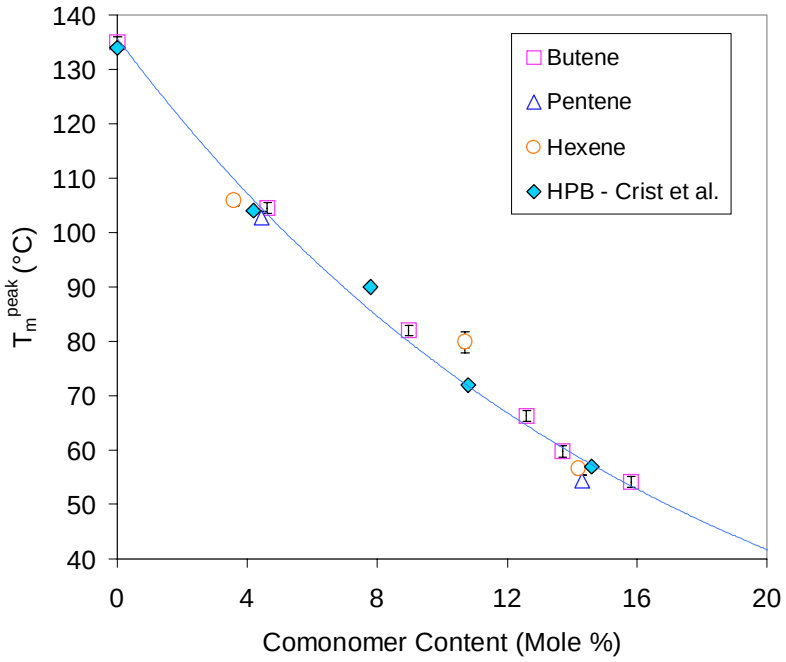

Figure 2 Peak melting temperatures for ethylene/1-butene, ethylene/1-pentene and ethylene/1-hexene copolymers as a function of comonomer content. The peak melting temperatures for HPBs[7] are also included.

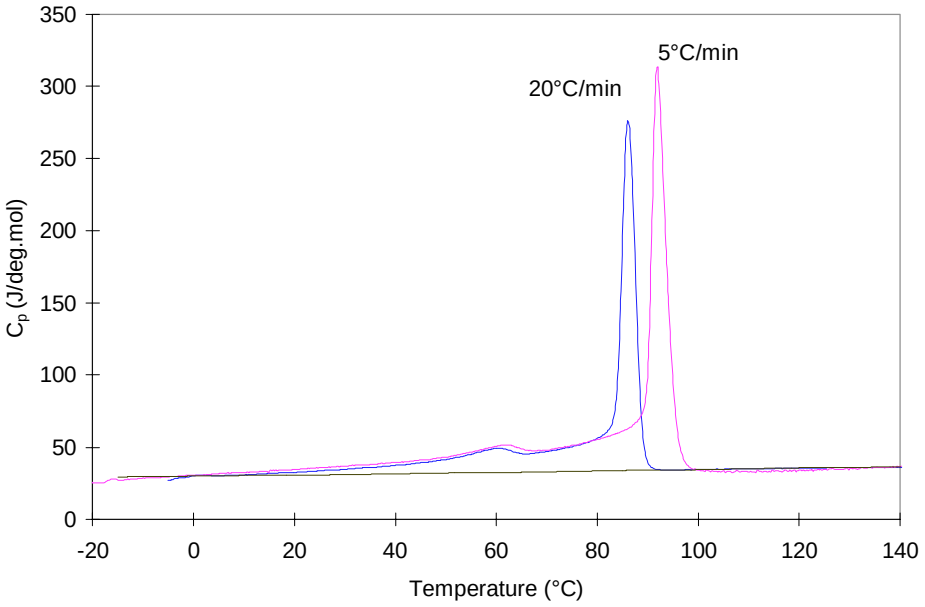

Figure 3 Corrected heat capacities for EB-912 during cooling from the melt at different rates

Partial areas were derived from these heat capacity curves and subsequently converted into degrees of crystallinity (χ_c) through the use of appropriate scaling factors, depending on the mass of the sample used. It is also noted there was no effect of sample mass on the results of the cooling experiments, within the range of sample masses (3-5 mg) utilized in the present study. Thus, the crystallinity values as a function of temperature, $\chi_c(T)$, were obtained for all the samples, at different cooling rates. The variation of χ_c with temperature for the various EB, EP and EH copolymers are shown in Figure 5, Figure 6 and Figure 7 respectively. The effect of cooling rate on the crystallization behavior of linear polyethylene (LPE) was reported as part of an earlier investigation carried out in this laboratory[21] and is shown in Figure 4.

In the case of LPE, the crystallinities display a strong cooling rate dependence at all temperatures.[22] Furthermore, the χ_c values increase significantly at high temperatures (during cooling), and appear to reach a nearly constant value extending over a broad temperature range (at the lower temperatures).

This is in sharp contrast to the trend exhibited by the copolymers. The crystallinity curves for these materials clearly depict the presence of two distinct regions of crystallization, demarcated by a cross-over temperature, T*. On the low temperature side of T*, the crystallinity values increase over a wide temperature range, while being cooling rate-independent. On the high temperature side, however, the crystallinities increase appreciably over a relatively narrow range and exhibit a strong dependence on cooling rate. The contribution of the increase in χ_c in the high temperature region to the total crystallinity is significantly larger for the lower branched materials. As the comonomer content is increased, this region becomes progressively less significant and becomes indiscernible beyond a certain branch content. The comonomer content also influences the cross-over temperature, T*, which systematically shifts to lower temperatures with increasing branch concentrations.

Another significant difference between LPE and the copolymers is the fact that the copolymer crystallinities continue to increase noticeably even at temperatures as low as -20°C, as opposed to the nearly constant values for LPE at such low temperatures. This observation is consistent with previous studies[4,23] whose results indicate that the level of crystallinity in such copolymers continues to increase appreciably until the glass transition temperature is reached. The degrees of crystallinity for the three types of copolymers at -20°C obtained from the crystallinity curves are plotted as a function of comonomer content in Figure 1. As discussed in Section 4.2, the crystallinity data for HPBs from the literature[6,7] are also included to verify the random statistics of the copolymers studied. The χ_c's for the copolymers are found to systematically decrease with increasing branch content, even at -20°C. This observation is directly related to the partitioning of the polymer backbone into shorter crystallizable segments by the branches.

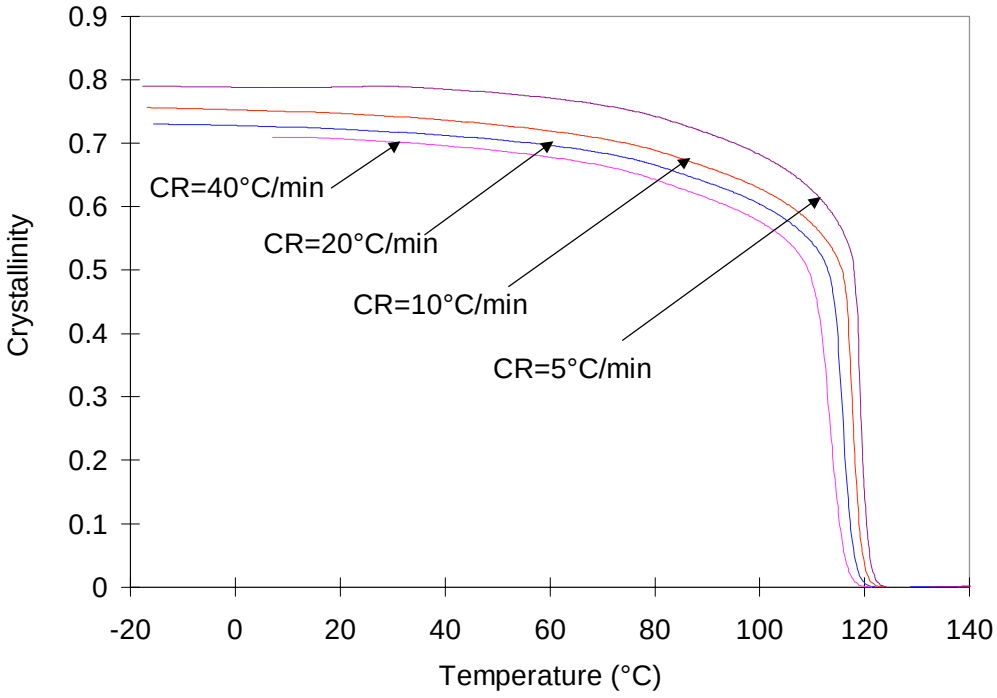

Figure 4 Degrees of crystallinity as a function of temperature obtained at different cooling rates from the melt for linear polyethylene (from Dr. A. Alizadeh)

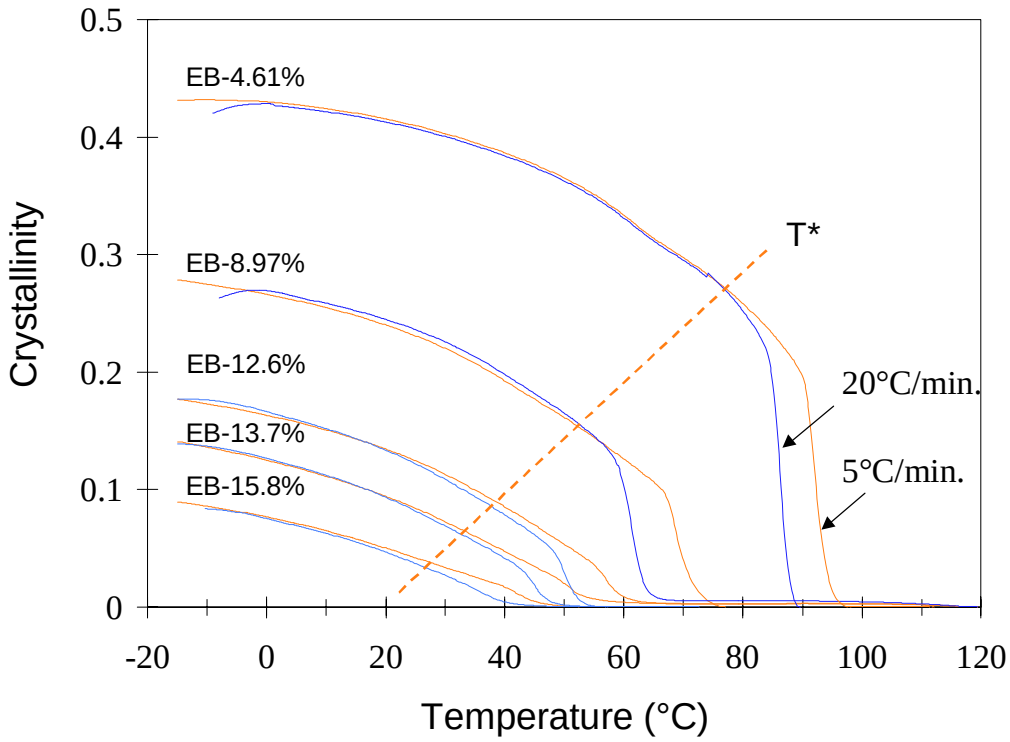

Figure 5 Degrees of crystallinity as a function of temperature obtained at different cooling rates from the melt for ethylene/1-butene copolymers of various branch contents

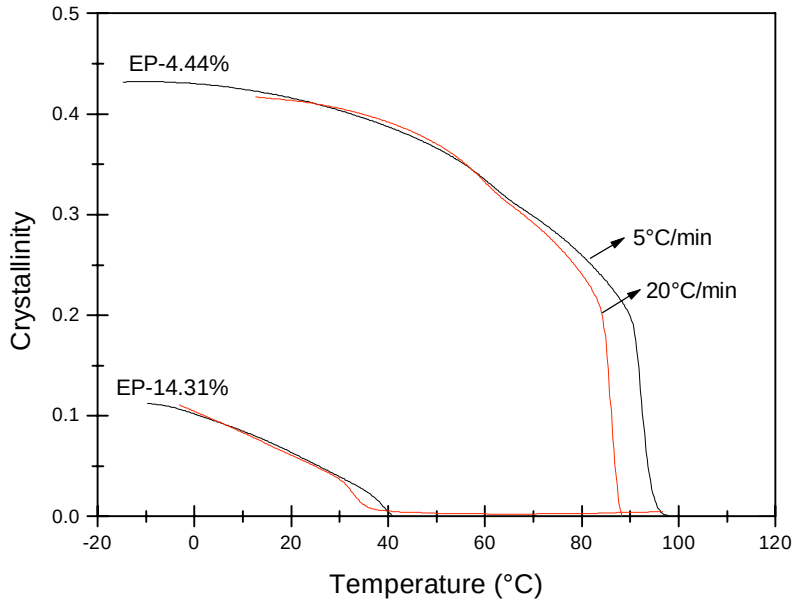

Figure 6 Degrees of crystallinity as a function of temperature obtained at different cooling rates from the melt for ethylene/1-pentene copolymers of various branch contents

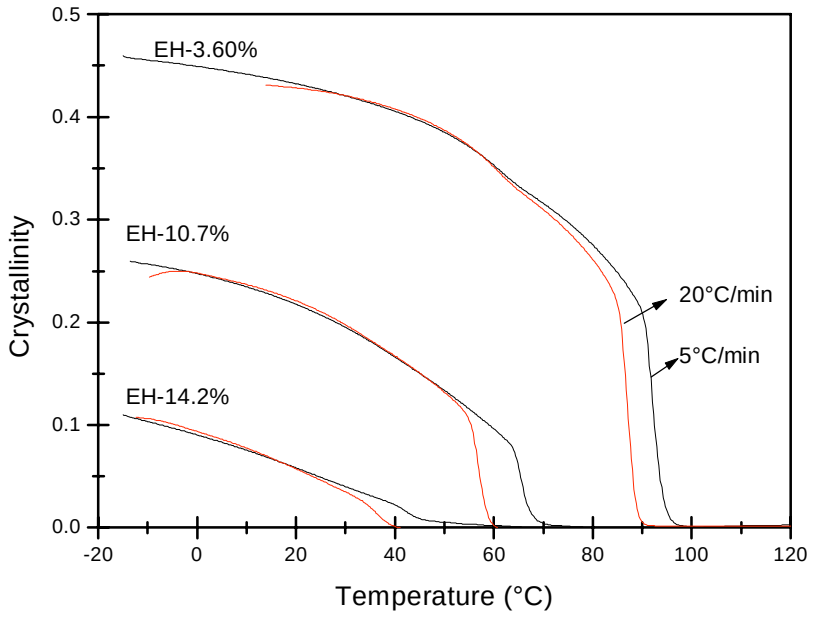

Figure 7 Degrees of crystallinity as a function of temperature obtained at different cooling rates from the melt for ethylene/1-hexene copolymers of various branch contents

5.4 Melting Behavior Subsequent to Crystallization during Cooling at Constant Rate

The reversibility of the crystallization and melting processes in the copolymers was investigated by obtaining the melting traces of the samples immediately after quenching from the melt to -20°C. The peak melting temperatures (T_m's) from the melting traces of the samples are plotted as a function of comonomer content in Figure 2. It is observed that T_m decreases progressively with increasing branch concentrations for all the copolymers studied.

The degrees of crystallinity calculated from the heating traces for EB-894 (with ~ 9 mole % branches) are plotted as a function of temperature in Figure 8. The $\chi_c(T)$ values estimated during the prior quenching of this sample from the melt to -20°C are also shown in the figure. Comparison of the two curves clearly indicate that the crystallinities obtained from the heating and cooling traces are identical to each other at low temperatures, and depart significantly from each other at higher temperatures. Two distinct regions of temperature dependence of the crystallinities are also found to exist. There is a high temperature region that exhibits a significant degree of hysteresis, and a lower temperature region with a remarkably reversible behavior. Similar observations were made on the other copolymers used in the present study, as well as on ethylene/1-octene copolymers that were studied previously in our laboratory[21]. It has been observed that the crystallinity change in the hysteretic region decreases progressively with increasing branch concentrations. This is parallel to the increase in the crystallinity change in the reversible region, with increasing comonomer content. Furthermore, the temperature delineating the two regions (hysteretic and reversible) is found to be identical to the temperature, T*, that marks the cross-over from a rate-dependence to a rate-independence of the degree of crystallinity from the cooling experiments. (Figure 5, Figure 6 and Figure 7).

This behavior of the copolymers discussed above is in sharp contrast to that of LPE. It has been demonstrated[21] that LPE predominantly exhibits hysteresis between the crystallinity curves derived from the crystallization and melting processes.

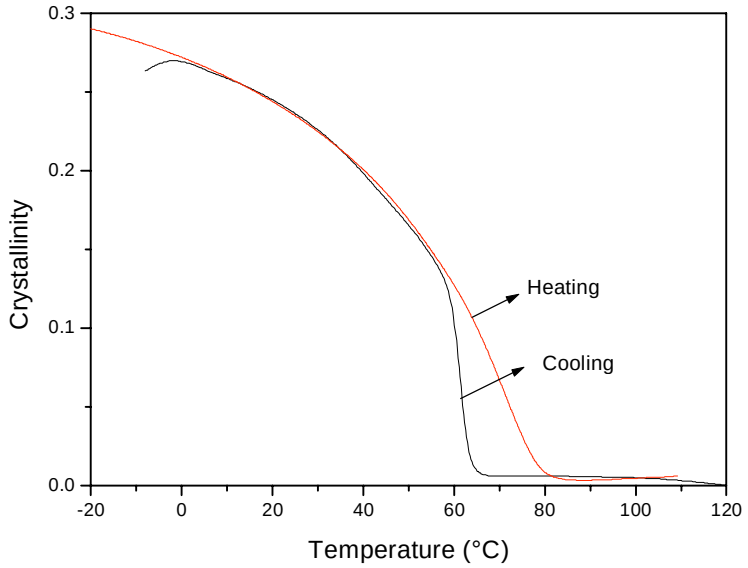

Figure 8 Degrees of crystallinity as a function of temperature for EB-894 during cooling at 20°C/min from the melt and during subsequent heating at 20°C/min.

5.5 Isothermal Crystallization at Room Temperature (~20°C) Subsequent to Quenching

From the two sets of experiments (cooling and heating) discussed above, it is clear that the temperature, T*, marks the transition between two regions of crystallization in the copolymers. The significance of this temperature will become more evident after discussing a model for the crystallization mechanism in such materials. However, at this point, it is important to recognize that the isothermal crystallization of a copolymer at temperatures above T* proceeds from a completely molten sample. In other words, this process could be characterized as primary crystallization. However, at temperatures below T*, the crystallization occurs from a partially crystallized material, i.e., secondary crystallization. Therefore, this temperature, T*, may also be viewed as the temperature at which crystallization is first observed during cooling, i.e., it is the temperature of incipient crystallization. The isothermal crystallization of the copolymers at various temperatures above and below T* was followed in the present study. This section is a discussion of the results obtained from the isothermal studies at T_x = 20°C, which is below the T* for all the copolymers examined. The results from the isothermal experiments at higher temperatures (including $T_x > T^*$) are discussed in the following section.

This series of experiments was designed to study the temporal evolution of the secondary crystallization process in the ethylene/α-olefin copolymers, at 20°C. The samples were quenched from the melt (160°C) to 20°C, and held at that temperature for times ranging from 1 minute to 6 months. They were subsequently quenched to -40°C, and then re-heated immediately at a rate of 10°C/min. to follow the melting behavior. The quenching and crystallization were carried out in the DSC itself, for most of the experiments (except for the very long times at room temperature, in which case the samples were crystallized in an oil bath held at that temperature). The heating traces collected for EB-883 after crystallization at 20°C for various times are shown in Figure 9. All the heating curves except for the one obtained after a direct quench from the melt display two distinct melting endotherms. The low temperature melting peak, which is referred to from now on as the "low endotherm" is seen to evolve approximately 5 to 20°C above the crystallization temperature. This peak increases in area and also shifts to

higher temperatures for longer crystallization times. A similar evolution of the low temperature endotherm was found in the melting traces of the other copolymers examined. The low endotherm observed here is comparable to the increases in specific heat observed slightly above the crystallization temperature by Mandelkern *et al*.[24] on very high molecular weight polyethylenes.

The high temperature melting peak, centered at ~ 70°C for the copolymer depicted in the Figure 9 is referred to as the "main endotherm". Both the position as well as the magnitude of this peak are found to be independent of crystallization time. However, they vary as a function of branch concentration within a given series of copolymers. It is also noted that the total heat of fusion, represented by the total area associated with the endothermic process in the temperature range between -40°C and the end of melting, also remains invariant with crystallization time.

A more subtle observation regarding the variation in heat capacity at lower temperatures (below the low endotherm) can also be made from the above figure. For the quenched material, a gradual melting is observed beginning as low as -30°C and extending all the way up to the main melting endotherm at ~ 70°C. However, with the evolution of the low endotherm at longer crystallization times, the heat capacity at the lower temperatures systematically decreases, as seen in the figure. This result implies that the fraction of material crystallizing during quenching below the crystallization temperature (here 20°C) is considerably reduced at longer times. The prolonged times at 20°C permit the chains that would have otherwise crystallized on subsequent quenching, to crystallize at that temperature.

The above result is exemplified by adopting a simple and direct approach to the analysis of the low endotherm. This was done by means of comparing the heating curves after different crystallization times to those after zero time, i.e., that of the quenched material. Accordingly, the melting traces of samples crystallized at 20°C for various times and subsequently quenched to -40°C (shown above) were subtracted from that of a sample directly quenched to –40°C from the melt. A series of typical subtracted curves for EB-883 are shown in Figure 10.

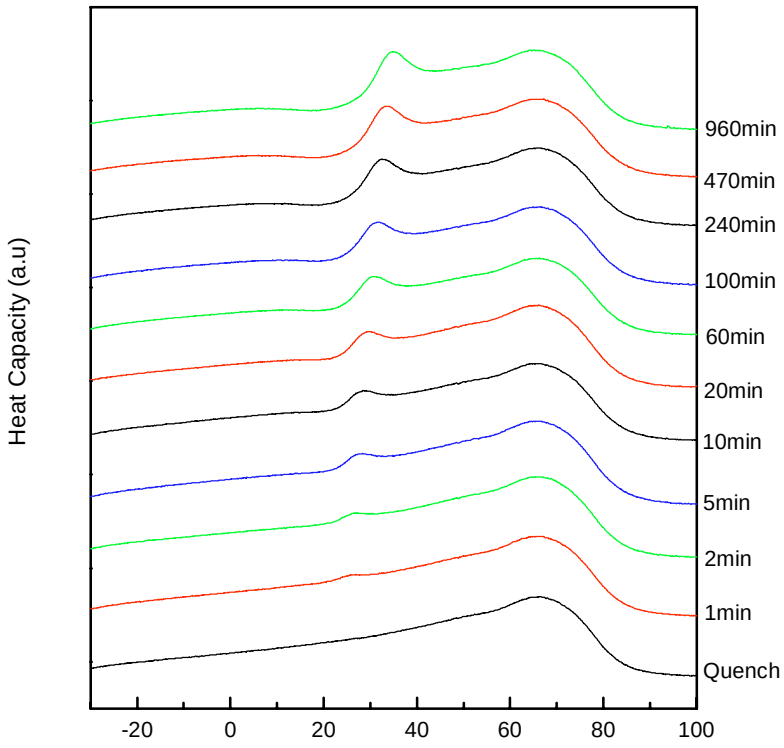

Figure 9 DSC thermograms for EB-883 after crystallization for various times at 20°C

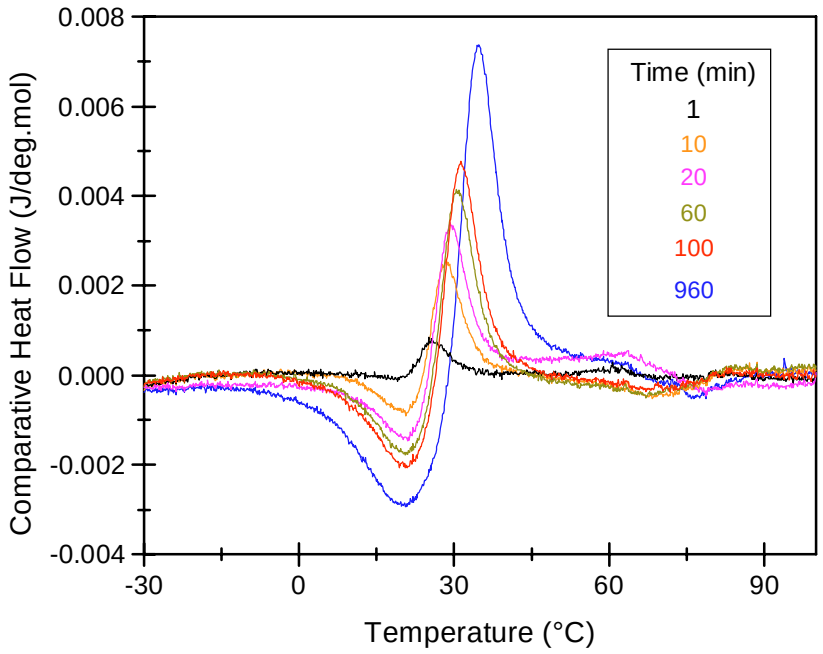

Figure 10 Curves obtained by subtraction of heating traces after finite crystallization times at 20°C from that of the quenched sample for EB-883

These curves consist of a heat flow contribution below $\Delta H_f = 0$ with a minimum centered around the crystallization temperature (20°C). The minima are associated with a reduction in the fraction of crystallizable material available during quenching below the crystallization temperature. The part of the curves above $\Delta H_f = 0$ is related to the evolution of the low endotherm, and exhibits maxima centered ~ 5 to 20°C above the temperature of crystallization. The magnitude of this positive deviation increases and its position shifts to higher temperatures at longer crystallization times, with a simultaneous increase in the magnitude of the negative deviation at ~ 20°C. These results suggest that the number of sequences available for crystallization during quenching below 20°C decreases significantly at longer crystallization times. Then, the evolution of the low endotherm at finite crystallization times may be visualized as occurring at the expense of another melting peak (rather a shoulder) that would otherwise be observed on directly quenching the samples from the melt to lower temperatures (below 20°C).

The positions and areas of the low endotherms in the heating traces were also determined using the curve fitting procedure described in Appendix I. This involved a careful deconvolution of the heating curves using an appropriate number of Gaussian peaks. An additional peak was included to represent the evolution of the lower endotherm with crystallization time. The position and magnitude of this peak were representative of the position and area of the lower endotherm. A series of such deconvoluted traces for EB-912 is shown in Appendix I. It must be noted that the positions and relative areas of the low endotherms estimated from the curve fitting procedure were found to be comparable to those calculated from the subtraction method described above, within the limits of experimental error.

5.5.1 Time Dependence of the Low Endotherm Location

The relative positions (T_m - T_x) where T_m = the observed low endotherm peak temperature and T_x = the crystallization temperature, of the low endotherms are plotted as a function of log crystallization time in Figure 11 for the sample, EB-912. [The error bars (in this and all subsequent plots) were estimated from the analysis of at least three

independent experimental traces]. The peak positions are found to increase linearly with the logarithm of crystallization time over the entire time scale examined. This linear relationship can be expressed as follows:

(1) $T_m - T_x = A + B \log t_x$

where t_x = the crystallization time

A and B are the intercept and slope from the linear regression, respectively.

Similar linear variations were observed for the evolution of the low endotherm with time, for the remaining ethylene/1-butene as well as the ethylene/1-pentene and ethylene/1-hexene copolymers studied, as depicted in Figure 12, Figure 13 and Figure 14 respectively. Furthermore, the data for all three types of copolymers can be superimposed on each other as shown in Figure 15. The fact that it is possible to represent all three copolymers by a single line, in spite of significant differences in their branch lengths further suggests that all three branch types may be completely excluded from the crystal lattice.

The experimental values of the constants, A and B for the copolymers are listed in Table 1 along with fit R^2 values. It is observed that the slope, B, has an average value equal to 3.0 ± 0.3°C. No particular trend in the values of the intercept, A, are observed. These values also appear to be independent of branch concentration and comonomer type. It is also noted that the low endotherm melting temperatures obtained at very short crystallization times coincide with the crystallization temperature. This implies that the crystals formed at short crystallization times melt at temperatures very close to the temperatures at which they were formed. Similar observations have been made in studies of ethylene/1-octene copolymers[21], PEEK[25] and PET[26] carried out in our laboratory.[27,28]

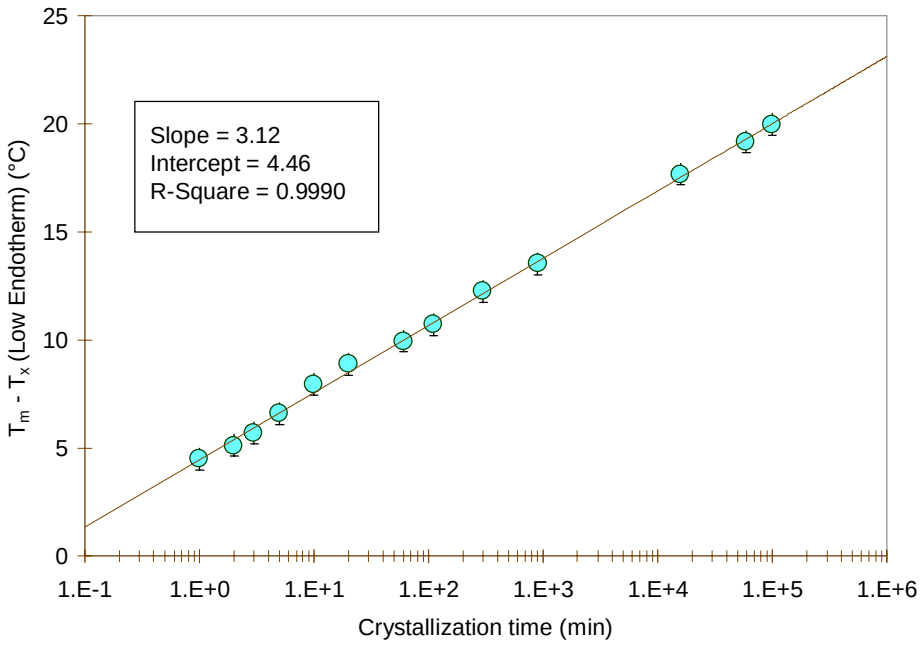

Figure 11 Relative positions of the low endotherms for EB-912 after crystallization for various times at 20°C

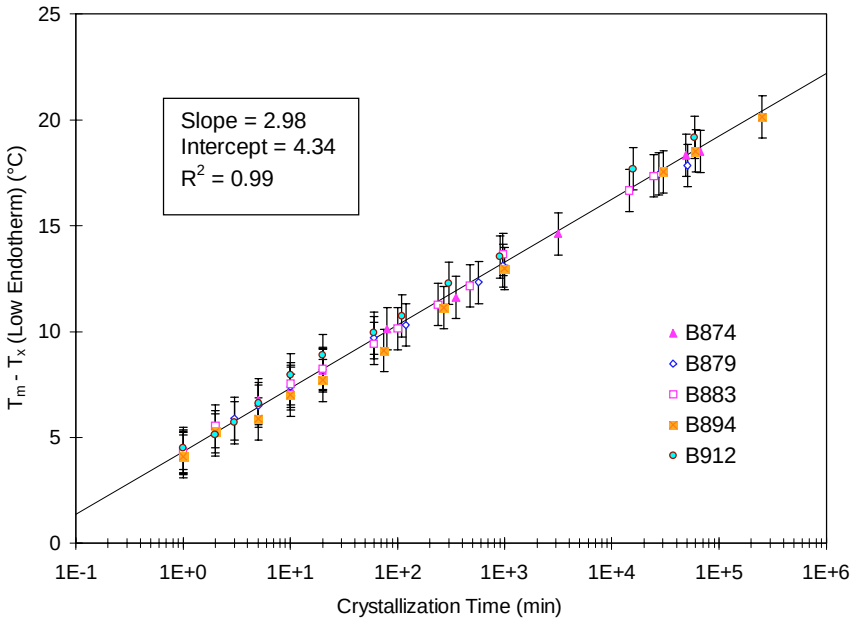

Figure 12 Relative positions of the low endotherms for ethylene/1-butene copolymers after crystallization for various times at 20°C

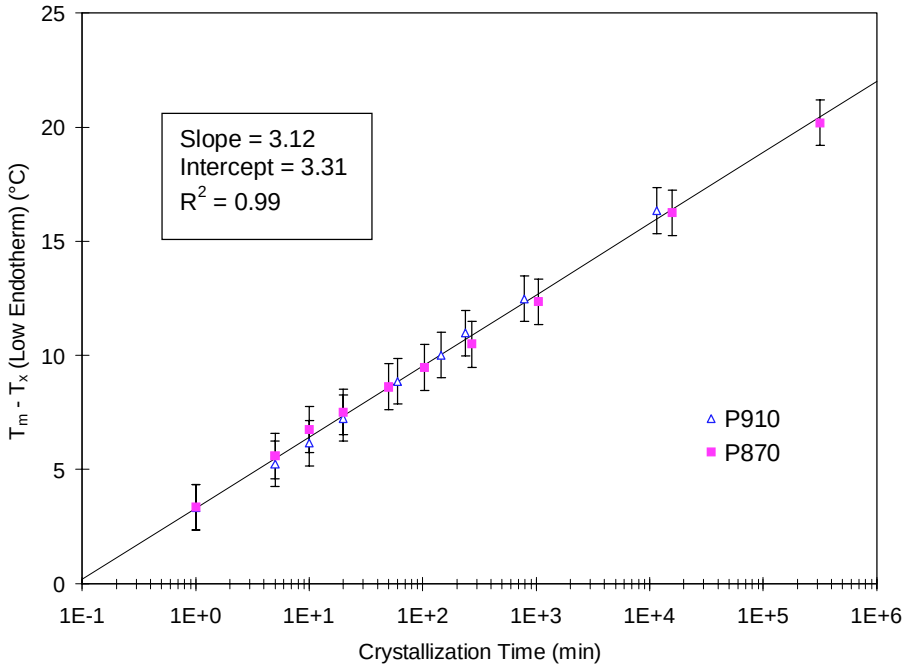

Figure 13 Relative positions of the low endotherms for ethylene/1-pentene copolymers after crystallization for various times at 20°C

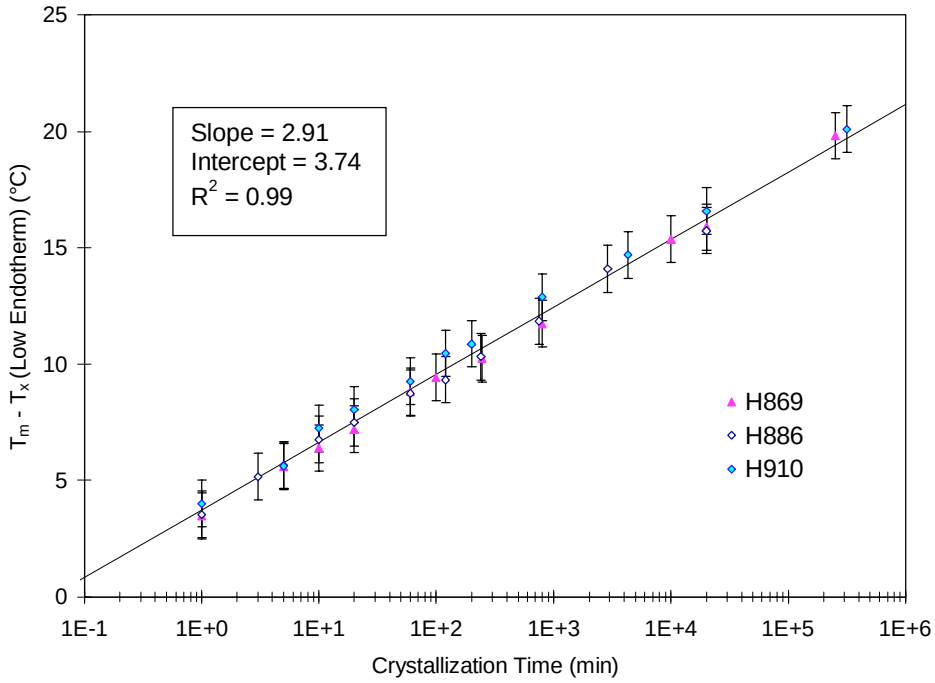

Figure 14 Relative positions of the low endotherms for ethylene/1-hexene copolymers after crystallization for various times at 20°C

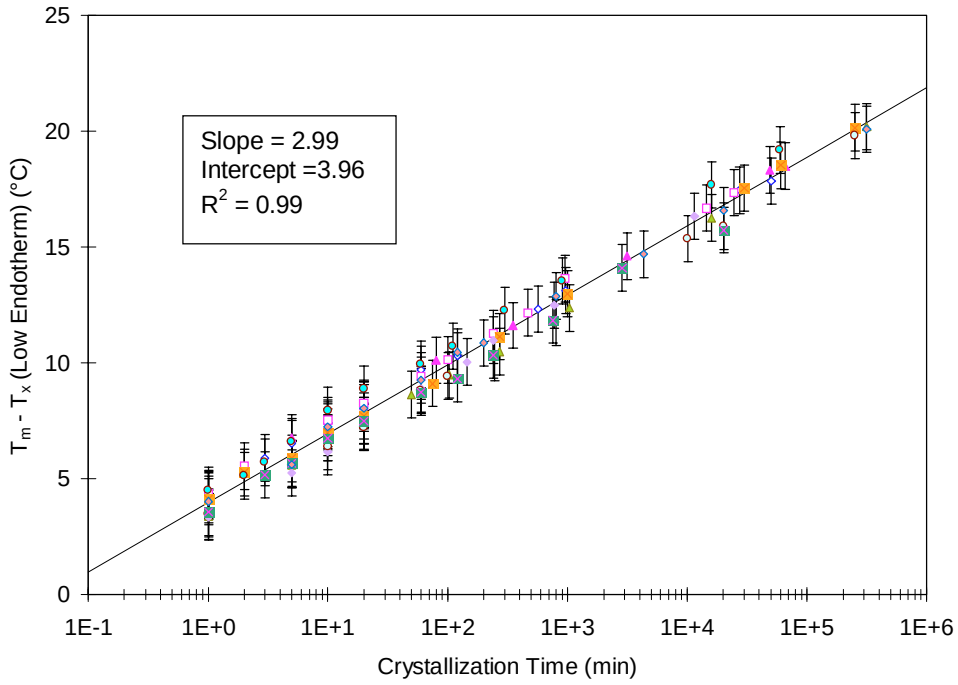

Figure 15 Relative positions of the low endotherms for ethylene/1-butene, ethylene/1-pentene and ethylene/1-hexene copolymers after crystallization for various times at 20°C

Table 1 The kinetic parameters, A, B, *n* and *k* and the degrees of crystallinity at -20°C and 20°C for the ethylene/α-olefin copolymers

Sample	A(°C)	B(°C)	R^2	χ_c (-20C)	χ_c(20C)	*n*	*k*
EB912	4.46	3.12	0.9990	0.43	0.42	0.46	0.10
EB894	3.93	3.02	0.9976	0.26	0.25	0.45	0.11
EB883	4.43	2.94	0.9977	0.18	0.14	0.47	0.12
EB879	4.44	2.89	0.9993	0.14	0.09	0.46	0.13
EB874	4.40	2.94	0.9988	0.09	0.05	0.45	0.12
EP910	3.10	3.25	0.9989	0.44	0.43	0.45	0.20
EP870	3.50	2.99	0.9978	0.12	0.07	0.42	0.10
EH910	3.65	3.30	0.9946	0.46	0.43	0.43	0.09
EH886	3.69	2.85	0.9963	0.26	0.21	0.45	0.20
EH869	3.51	2.90	0.9986	0.11	0.06	0.40	0.23

5.5.2 Avrami Equation

In this study, the temporal evolution of the enthalpies of fusion of the low endotherms was modeled using a double logarithmic plot. Such a representation is based on the Avrami equation in the context of the free growth approximation. It is useful to briefly review the underlying theory before proceeding with the details of the enthalpy analysis.

5.5.2.1 Theory

The theoretical as well as experimental aspects related to the crystallization of homo- and copolymers of ethylene were discussed in Chapter 2. It is clear from that discussion that the equilibrium relationships proposed are satisfied only to a very limited extent in polymer crystallization, the main reason being the restrictions imposed by the kinetic factors involved with the process. A better understanding of these factors can be gained by studying the rates and mechanism of crystallization in the samples. In the present study, this was achieved by adopting an Avrami-type analysis of the heats of fusion. The important aspects of this type of analysis are presented below.

The Avrami equation[29,30,31] was originally derived based on the theory that the emergence of a crystalline phase in a semicrystalline polymer occurs via two steps:

1. Initial formation of a nucleus or a growth center as a result of random fluctuations in the bulk liquid (homogeneous nucleation) or at the interface of foreign bodies (heterogeneous nucleation).
2. Subsequent growth of the above nuclei determined by factors including temperature, chain mobility etc.

A number of different crystallization mechanisms were considered and an equation of the form shown below, common to all of them, was obtained.

(2) $$\theta_r(t) = 1 - \exp(-Kt^n)$$

where $\theta_r(t)$ = the relative crystallinity at time *t*

n = the Avrami exponent, and

K = the Avrami rate constant.

The relative crystallinity, θ_r, at any time, *t* is given by the ratio of the crystallinity at that time to that at the end of crystallization, i.e., $t = \infty$, as shown below.

$$\theta_r(t) = \frac{\theta_c(t)}{\theta_c(\infty)}$$

The rate constant, K, is a cluster of numerical and growth constants, and provides information regarding the growth rate, G, and the nucleation density, N. For instance, in the case of a predetermined nucleation of growth centers followed by a three-dimensional growth of crystallites, the rate constant, K, is given by the expression,

$$K = \frac{4}{3}\pi G^3 N$$

The exponent, *n*, expresses the power dependence on time of the crystallization process, and can assume integral as well as non-integral values ranging from 0.5 to 4[32,33]. The value of this exponent is directly related to the processes governing the nucleation and growth mechanisms,[34] some of which are listed in Table 2. It is evident from this table that there exists a multitude of possibilities for the crystallization mechanism in a selected polymer, depending on the crystallization conditions. Although the values of the exponent derived from a few different mechanisms are identical to each other, the method of using the Avrami exponent as a means of characterizing the crystallization process is still valuable. This is particularly true in instances where the processes of crystallization in two or more samples or in a given sample under different conditions, are compared to each other. In the present study, the behaviors during the crystal formation of the copolymers with three different branch types were compared to each other. Furthermore, for a given branch type the variations with differing branch concentrations and

crystallization temperatures as well as times were considered. Therefore, the use of the Avrami method in such an analysis can provide useful information regarding the crystallization behaviors of the copolymers.

Equation (2) can be rearranged as follows:

$$\frac{1}{1-\theta_r(t)} = \exp\left(Kt^n\right)$$

Obtaining the double logarithm of the above expression yields,

(3) $$\ln(-\ln(1-\theta_r(t))) = \ln K + n \ln t$$

Thus, a straight line is obtained on plotting $\ln\left(-\ln\left(1-\theta_r(t)\right)\right)$ vs. ln *t*. The slope and intercept of this line yield the values of the exponent, *n*, and the rate constant, K, respectively.

For relatively small extents of crystalline transformation, the Avrami formulation is identical to the free-growth approximation of Göler *et al.*[35] and is given as:

(4) $$\theta_r(t) = Kt^n$$

or alternatively as $\Delta H = Kt^n$. Obtaining the logarithm on both sides of this equation yields:

(4') $$\log(\theta_r(t)) = \log K + n \log t$$

$$\log(\Delta H) = \log K + n \log t$$

A double logarithmic representation based on this expression i.e., log (ΔH) vs. log (time) was employed in the present study to examine the kinetics of copolymer crystallization.

The kinetic parameters, *n* and K, were obtained from the slope and intercept of this plot, respectively.

5.5.2.2 Assumptions

It is also important to realize the limitations of the analysis of the type presented above. The original derivation of the Avrami equation was based on the following assumptions.

1. That the growth rate as well as the shape and density of the growing macrostructure are constant. This assumption is especially significant in view of the nature of the secondary crystals being examined in the present study.
2. That a single mode of nucleation is involved. This assumption is particularly relevant to the isothermal crystallization conditions used in the present study. Under such conditions, mixed nucleation modes may be expected.

However, in the current study, these limitations were kept to a minimum due to the following reasons. The Avrami-type analysis used in the present study is based on the assumption that the composition and structure of the melt remains invariant during the course of the crystallization.[36,37,38] In the case of the secondary crystallization of the ethylene/α-olefin copolymers, relatively small extents of transformation are involved. Therefore, the residual melt surrounding the secondary crystals does not vary in composition as much as during primary crystallization.

Furthermore, it is known from the cooling experiments that different copolymers (with varying branch contents) develop different crystallinities on quenching from the melt to a crystallization temperature. Therefore, it would be incorrect to directly compare the crystallization rates, K, for the different samples, derived from the Avrami analysis. In order to remedy this discrepancy, the heats of fusion of the low endotherm at any crystallization time (and temperature) were normalized with respect to the initial amorphous content at the beginning of isothermal crystallization, i.e., $t_x = 0$, at that temperature. This process resulted in a normalized rate constant, *k*, for the samples.

Table 2 Avrami exponents and associated crystal geometries for different crystallization mechanisms (Adopted from Ref. 32)

Avrami Exponent	Crystal Geometry	Nucleation Mode	Rate Determination
0.5	Rod	Simultaneous	Diffusion
1	Rod	Simultaneous	Nucleation Controlled
1	Disk	Simultaneous	Diffusion
1.5	Sphere	Simultaneous	Diffusion
1.5	Rod	Sporadic	Diffusion
2	Disk	Simultaneous	Nucleation Controlled
2	Disk	Sporadic	Diffusion
2	Rod	Sporadic	Nucleation Controlled
2.5	Sphere	Sporadic	Diffusion
3	Sphere	Simultaneous	Nucleation Controlled
3	Disk	Sporadic	Nucleation Controlled
4	Sphere	Sporadic	Nucleation Controlled

[The normalized constant, *k*, and not K from the previous equations, will be used from now on]. A comparison of this normalized value for the different copolymers yields useful information regarding their kinetics of crystallization. The details of the normalization procedure are discussed in a following section (Section 5.5.3.2).

Thus, the Avrami-type analysis in the present study provides useful information about the mechanism of the crystallization process involved. It also serves as a means of comparing crystallization mechanisms in the different copolymers, when crystallized under the same or different conditions.

5.5.3 Analysis of the Crystallization Time Dependence of the Low Endotherm Enthalpy

5.5.3.1 Avrami Exponents

The log of the heat of fusion of the low endotherms varies linearly with log (t_x) at short crystallization times, i.e., $\Delta H = kt^n$ as shown in Figure 16 for EB-912. The slopes, *n*, and intercepts, *k*, at 20°C for all the ethylene/α-olefin copolymers studied are listed in Table 1. It is found that the values of *n* are close to 0.5 for all the samples, independent of branch type or concentration. A value of $n = 0.5 \pm 0.1$ was also obtained in a parallel study of ethylene/1-octene copolymers carried out in our laboratory.[21] It was mentioned earlier that the value of *n* is a function of the type of nucleation, say homogeneous or heterogeneous. For nucleation-controlled growth processes, *n* is related to the morphology of the polymer as follows:

n = 3 represents a 3-dimensional spherulitic morphology

n = 2 represents a 2-dimensional disc-like superstructure, and

n = 3 represents a 1-dimensional diffusion controlled growth.

The value of *n* = 0.5 obtained in the present study is suggestive of a one-dimensional diffusion-controlled mechanism for the secondary crystallization, as opposed to the normal nucleation and growth leading to a three-dimensional spherulitic morphology.

A significant deviation from the power law described above was observed immediately after the initial linear increase of ΔH. Subsequently, the heats of fusion begin to exhibit a weak linear variation with log (t_x) at times longer than ~ 900 minutes, as shown in the bottom part of Figure 16.

This increase is, however, very slow and insignificant compared to the initial linear increase and appears as an apparent plateau in the figures. The heat of fusion corresponding to the apparent plateau is found to vary systematically as a function of comonomer composition. Thus, these results indicate the existence of two distinct regions of temporal variation of the secondary crystallization in the ethylene/α-olefin copolymers.

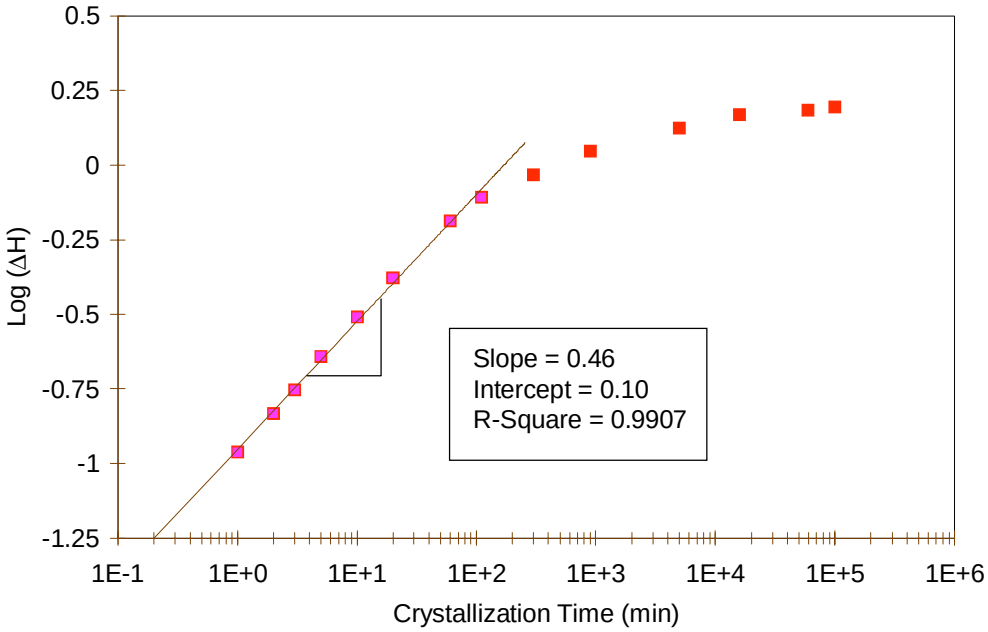

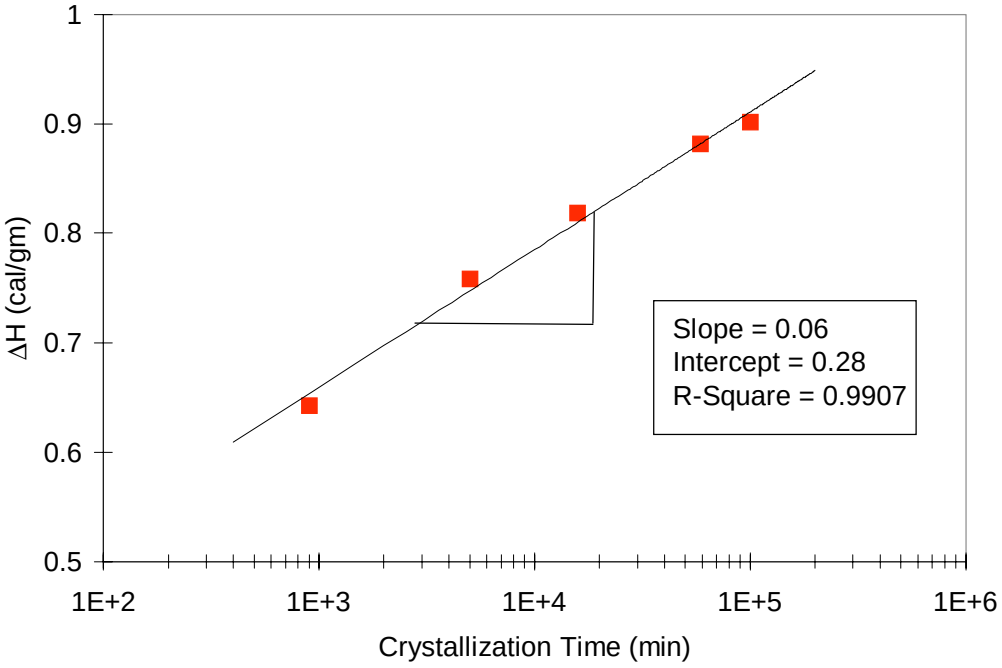

Figure 16 Typical Avrami plot for EB-912 after crystallization for various times at 20°C. The parameters corresponding to short (top) and long (bottom) times are also indicated

5.5.3.2 Crystallization Rate Constants

It has been demonstrated that kinetic information may be obtained from the heats of fusion based on an Avrami-type analysis.[39,40,41,42] [The Avrami intercept, K is directly related to the crystallization rate constant of the sample]. In the present study, the crystallization rates were estimated from the intercept, K of the double logarithmic plots. A simple comparison of the intercepts obtained from the plots was not possible due to the fact that different copolymers (with varying branch contents) develop different crystallinities on quenching from the melt to the crystallization temperature. The values of crystallinity, prior to isothermal crystallization at 20°C were obtained from the crystallinity vs. temperature plots (constructed from the cooling traces) described in Section 4.3. The corresponding amorphous fraction at 20°C was evaluated from the initial values of χ_c based on a two-phase model of semicrystalline polymers.[34,43,44] The heats of fusion of the low endotherm at any crystallization time were normalized with respect to the initial amorphous content at the beginning of isothermal crystallization i.e., $t_x = 0$. It is these normalized values that were used in the Avrami-type analysis. The crystallization rate constants, *k* for all the copolymers, estimated from the normalized plots are listed in Table 1. The *k* values thus obtained are plotted as a function of comonomer content for the ethylene/1-butene copolymers in Figure 17. A maximum at ~ 13 mole % 1-butene is observed.

It may be recalled that two distinct regions of crystallization were observed for the copolymers by means of the cooling experiments, a low temperature cooling rate-independent region and a high temperature rate-dependent region separated by the transition temperature, T*. In the above section, the results from isothermal crystallization studies at 20°C for the ethylene/α-olefin copolymers were reported. This temperature lies in the cooling rate-independent region (below T*) for all the samples. Isothermal experiments have also been done at several other temperatures. The results from those experiments are discussed in the following section.

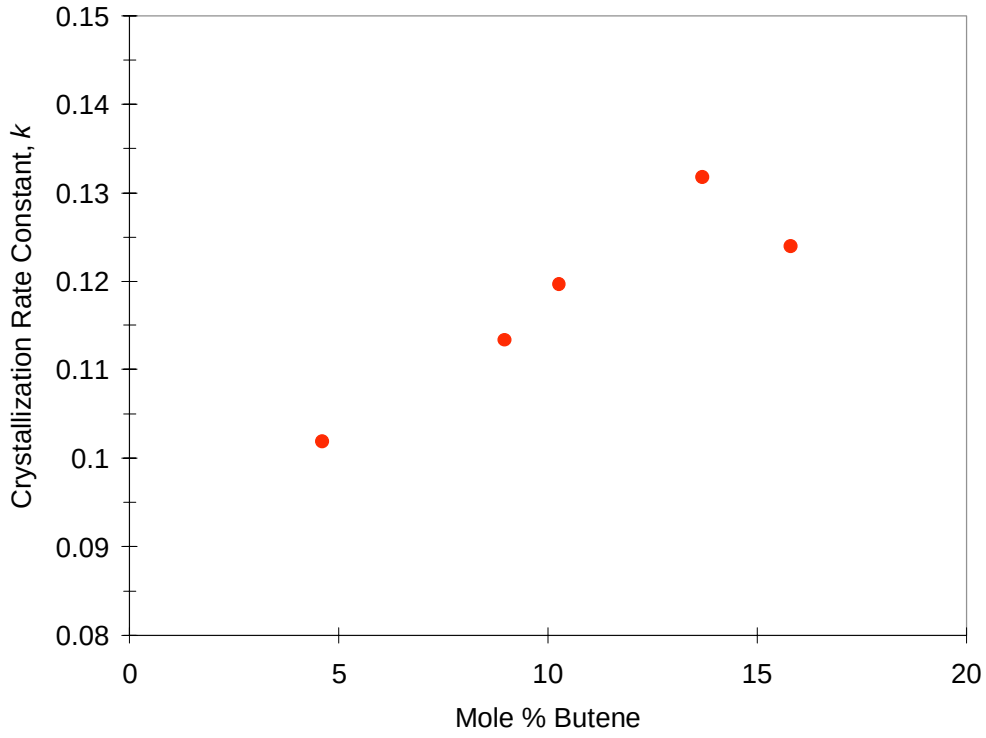

Figure 17 Crystallization rate constant, *k* as a function of branch concentration for ethylene/1-butene copolymers

5.6 Isothermal Crystallization at Higher Temperatures

5.6.1 Influence of Crystallization Temperature

These experiments were similar to the isothermal study at 20°C. The samples were held in the melt (160°C) for 2 minutes, and then quenched to the crystallization temperature (T_x). They were crystallized at that temperature for various times (t_x) and subsequently quenched to -20°C. Their melting endotherms were obtained immediately after quenching, at a heating rate of 10°C/minute. The crystallization temperatures selected for the ethylene-1-butene copolymers ranged from 30 to 100°C. The maximum temperature for a given copolymer was determined by its branch content, ranging from 60°C for a copolymer with ~ 16 mole % butene comonomer, to 100°C for a copolymer with ~ 5 mole % butene comonomer. A typical set of melting traces obtained for EB-912 after crystallization for long times (t_x > 1000 min.) at T_x's ranging from 20 to 100°C is shown in Figure 18. A clear distinction can be made between the thermograms above and below T_x = 80°C. The heating curves obtained at $T_x \leq 80$°C are similar to those obtained at T_x = 20°C (shown in Figure 9 for EB-883), with respect to the number and nature of the endotherms involved. However for T_x > 80°C, a significant change in the shape of the thermogram is observed, including the merging of the "low endotherm" with the main melting peak. This observation is directly related to the fact that the isothermal crystallization at T_x > 80°C occurs from a completely molten (liquid) sample, whereas that at $T_x \leq 80$°C occurs from partially crystallized material. This can be further verified by referring to the crystallinity vs. temperature curves for this copolymer, shown in Figure 5. A direct implication of the above observation is that a finite induction time exists before the initiation of crystallization at T_x > 80°C. However, for $T_x \leq 80$°C, a low endotherm is detected even at crystallization times as short as 1 minute. It is also noted that T_x = 80°C, where the above distinctions begin to be discerned is identical to the cross-over temperature, T*, that marks the transition between cooling rate-dependence to rate-independence of $\chi_c(T)$, for this copolymer

The existence of a finite induction time for EB-912 at T_x = 100°C (> 80°C) is evident in Figure 19. This figure is a plot of the melting traces of EB-912 obtained after

crystallization at 100°C for various times. The presence of an endotherm above T_x is not detected for crystallization times below t_x=50 min.

5.6.2 Crystallization Time Dependence of the Endotherm Peak Location

The location and heat of fusion of the endotherms associated with the melting of crystals formed at T_x for different t_x's were obtained by the deconvolution process described earlier. The peak positions of the endotherms for EB-912 at crystallization temperatures ranging from 20 to 100°C are plotted as a function of log crystallization time in Figure 20. A linear variation of the endotherm position with log (t_x), following a relationship of the type shown in Equation (1) is observed at all the crystallization temperatures. The slopes, B, and intercepts, A, corresponding to these lines are listed in Table 3. It is obvious from the figure that the lines corresponding to crystallization temperatures below 80°C are much steeper than those for the higher temperatures. Accordingly, the values of B for $T_x < 80$°C vary closely around 3.0, whereas for $T_x \geq 80$°C, they are considerably reduced and approach the value reported for linear polyethylene[45]. This variation in slope, B, is accompanied by a change in the temperature reached on extrapolation of the endotherm position to very short times (of the order of a few seconds). For $T_x < 80$°C, such an extrapolation always yields the crystallization temperature (T_x), whereas for $T_x \geq 80$°C, the extrapolated value is higher than T_x.

5.6.3 Avrami-Type Analysis of the Heat of Fusion

Heats of fusion associated with the crystallization at different T_x's were estimated following the deconvolution process already described. A plot of log(ΔH) vs. log(t_x) for EB-912 at three different crystallization temperatures is shown in Figure 21. The slopes, *n*, and crystallization rate constants, *k*, are listed in Table 3. An initial linear variation is observed at all temperatures with the slopes, *n*, varying closely around 0.5 for $T_x < 80$°C. However for higher T_x's the values of *n* are found to increase significantly with temperature.

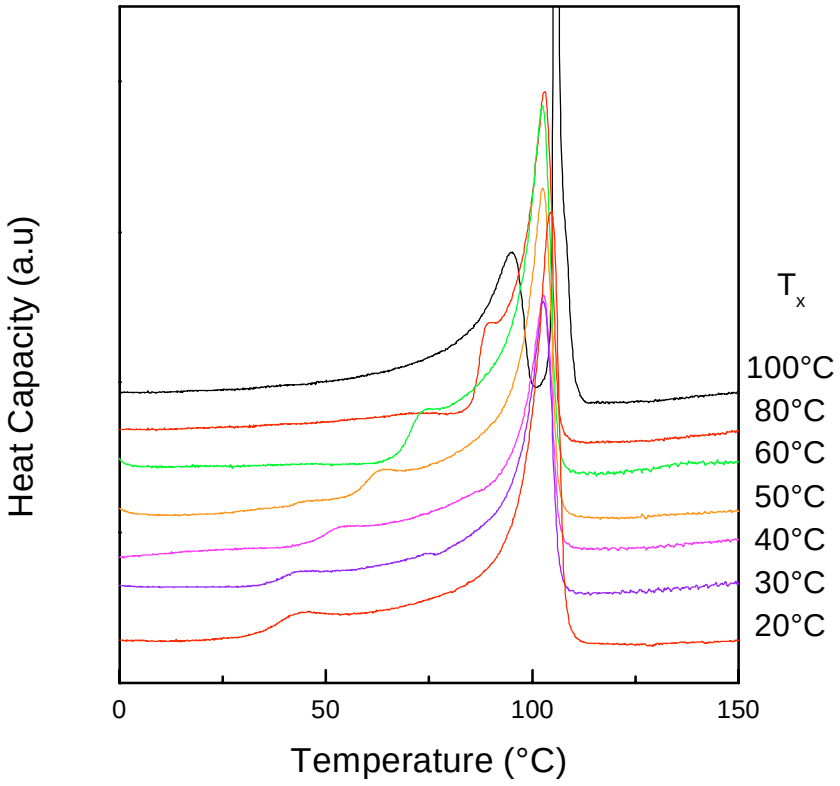

Figure 18 DSC thermograms for EB-912 after crystallization for long times at different crystallization temperatures

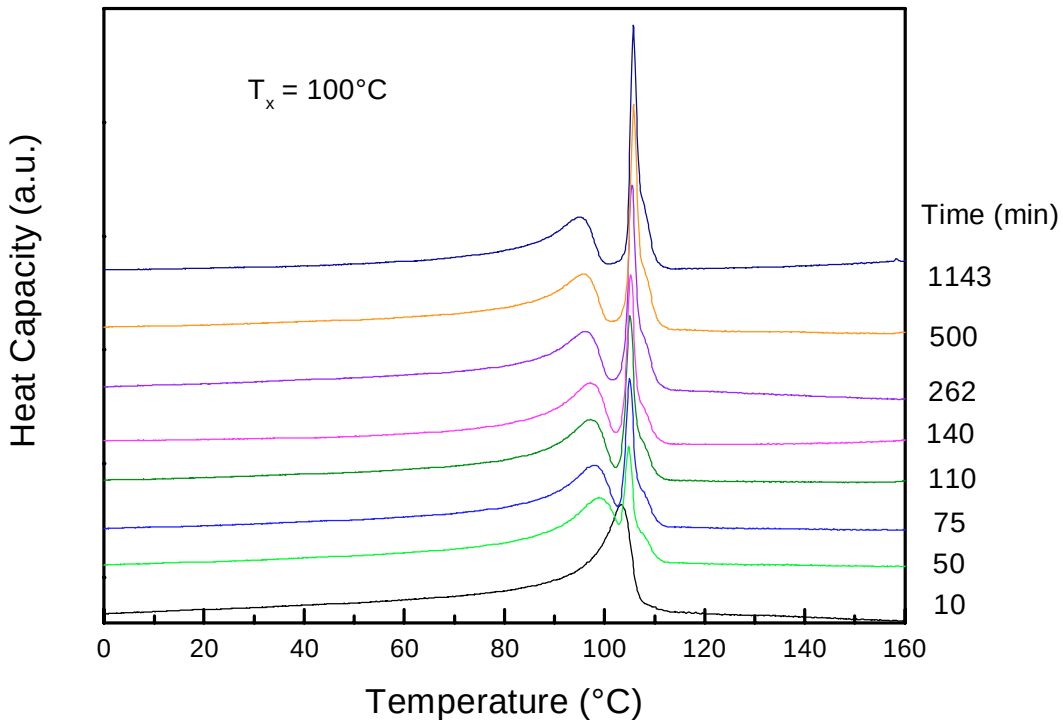

Figure 19 DSC thermograms for EB-912 after crystallization for various times at 100°C

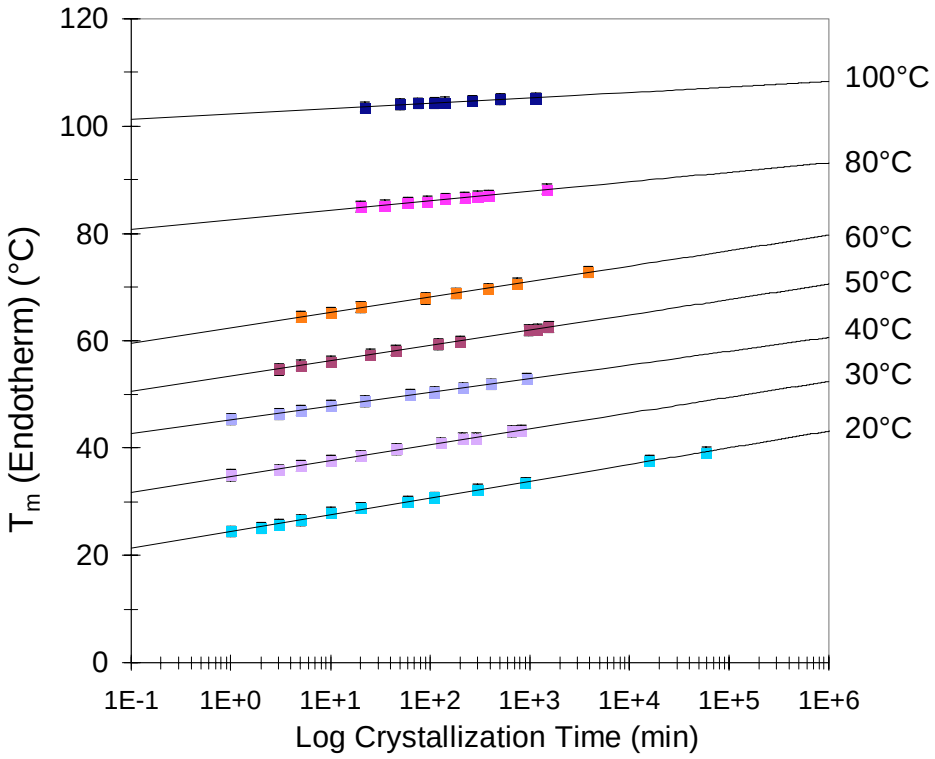

Figure 20 Peak positions of the endotherms for EB-912 after crystallization at various times for T_x ranging from 20 to 100°C

Table 3 The parameters, A, B, *n* and *k* and the degrees of crystallinity at T_x for EB-912 crystallized at various temperatures (T_x) from 20 to 100°C

T_x (°C)	A (°C)	B (°C)	R^2	χ_c	*n*	*k*
20	4.46	3.12	0.9980	0.42	0.46	0.10
30	3.78	2.96	0.9968	0.40	0.46	0.25
40	4.41	2.56	0.9985	0.39	0.47	0.75
50	2.64	2.81	0.9991	0.37	0.47	0.29
60	2.38	2.88	0.9975	0.33	0.47	0.13
80	2.71	1.68	0.9837	0.26	0.57	0.10
100	2.27	0.99	0.9800	0.01	1.09	0.07

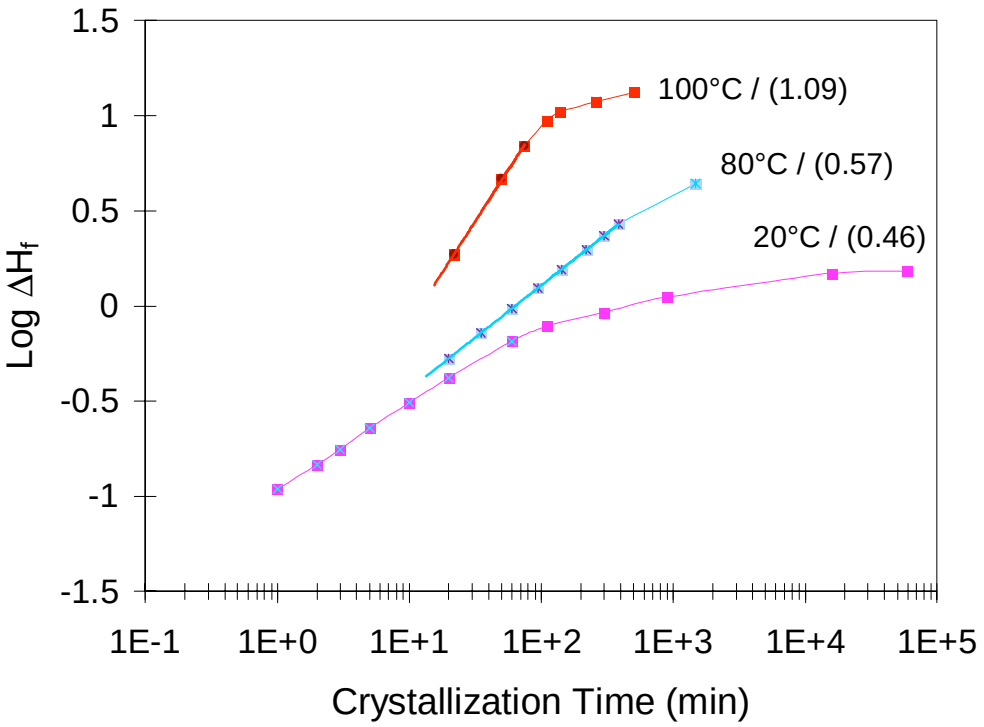

Figure 21 Avrami plots for EB-912 (with ~ 5 mole % butene) crystallized at various temperatures. The numbers indicate $T_x/(n)$.

It was mentioned earlier that the Avrami exponent, *n* , is related to the morphology of the polymer. It is widely believed that an exponent value of 3-4 is representative of nucleation controlled growth, leading to a 3-dimensional spherulitic morphology. Such values have been reported for the crystallization process in linear polyethylene[46]. The value of 0.5 obtained at $T_x < 80°C$ for EB-912 in the present study could be related to a 1-dimensional diffusion controlled growth process with athermal nucleation. Similar values for the Avrami exponent have been reported by Schultz and Scott[47] for the secondary crystallization of linear polyethylene after cooling to temperatures below that of primary crystallization. These authors have indicated that a value of $n = 0.5$ is consistent with the predictions of "instantaneous nucleation" and "diffusion controlled one-dimensional growth". They have also extended their observation to suggest that it could be related to previous observations[48] of bridge-like links between the edges of chain folded lamellar crystals.

It is also important to recognize that the increase in the exponent values for EB-912 begins to occur at ~ 80°C, which is identical to the temperature at which the sharp change in the slope, B, was found to occur, as discussed in Section 4.5.4.2. This temperature is also consistent with the transition temperature (T*) for this copolymer, obtained from the crystallinity curves of Figure 5.

The crystallization rate constants listed in Table 3 for EB-912 are found to be temperature dependent. These values have been normalized with respect to the initial amorphous content (as described in Section 5.5.3.2), in view of the fact that a given copolymer develops different degrees of crystallinity on being quenched from the melt to different crystallization temperatures. The initial crystallinity values at T_x required for this normalization were obtained from the χ_c vs temperature plots for the copolymer. The normalized rate constants, *k*, for EB-912 are plotted as a function of crystallization temperature in Figure 22. A bell-shaped curve with a maximum at ~ 40°C is obtained. This shape can be interpreted as follows. The mobility of the chain segments decreases while approaching the glass transition temperature of the copolymer. As a result, the growth rate decreases with decreasing temperature (while approaching T_g). At temperatures closer to the melting temperature, crystal growth is limited by nucleation, thereby causing the growth rate to increase with decreasing temperatures[33,49] (while

moving farther from T_m). A maximum in the curve occurs when a balance between the two opposing factors is achieved.

5.6.4 Variation of Kinetic Parameters Above and Below T*

The above discussion was mainly focused on the influence of crystallization temperature and time on the crystallization of EB-912. Similar trends were observed for all the copolymers examined. The variation in the slope, B, as a function of crystallization temperature for three different ethylene/1-butene copolymers is plotted in Figure 23. The temperatures (for the three samples) at which the values of B begin to display temperature dependence (from B = 3) is indicated by the arrows in the figure. A similar plot depicting the variation of the Avrami exponents, *n*, for the same copolymers is shown in Figure 24. As before, the temperatures at which the values of *n* begin to exhibit temperature dependence (from $n = 0.5$) is indicated by the arrows, for the three copolymers. It is important to mention that the lines depicted in both the figures merely serve as visual guides and bear no physical significance. For a given copolymer, the temperatures marked by the arrows in the two figures are identical to each other. Furthermore, this temperature is the same as the cross-over temperature, T*, at which the transition from cooling rate-dependence to rate-independence occurs in the χ_c vs. temperature curves. As clearly seen from these figures, this temperature is strongly dependent on the comonomer content of the copolymer.

So far, the results of the thermal analysis studies on ethylene/α-olefin copolymers have been reported. The crystallization temperature dependence in the case of ethylene/1-butene copolymers was discussed in detail. A discussion of these results is presented in the following section.

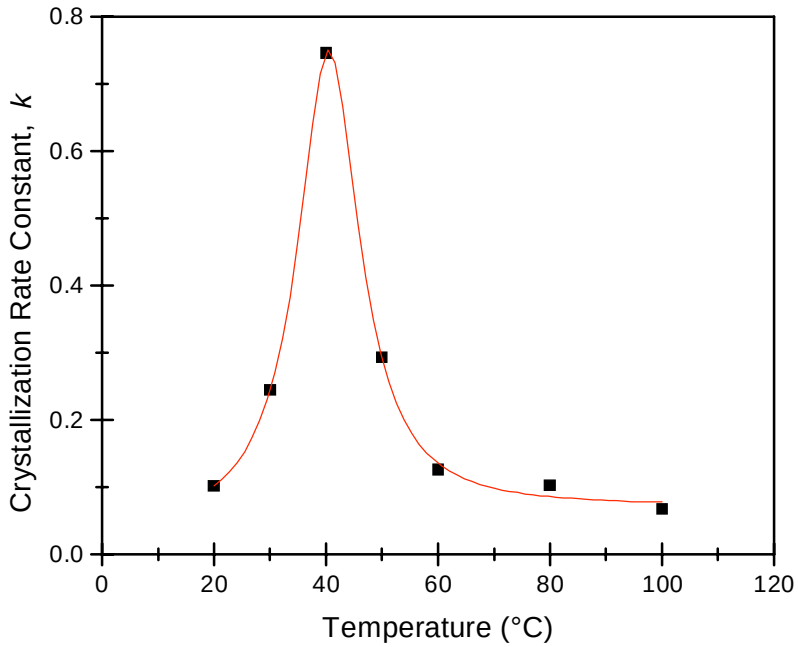

Figure 22 Normalized rate constant, *k*, for EB-912 as a function of crystallization temperature

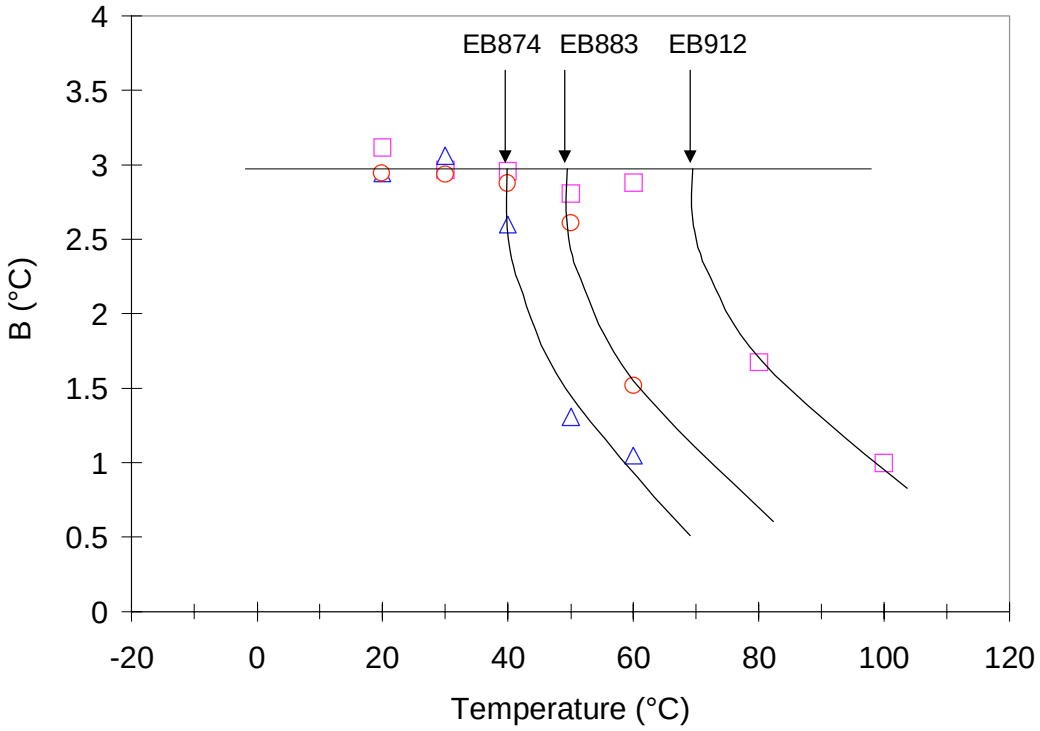

Figure 23 Variation of B as a function of crystallization temperature for the ethylene/1-butene copolymers of various branch contents

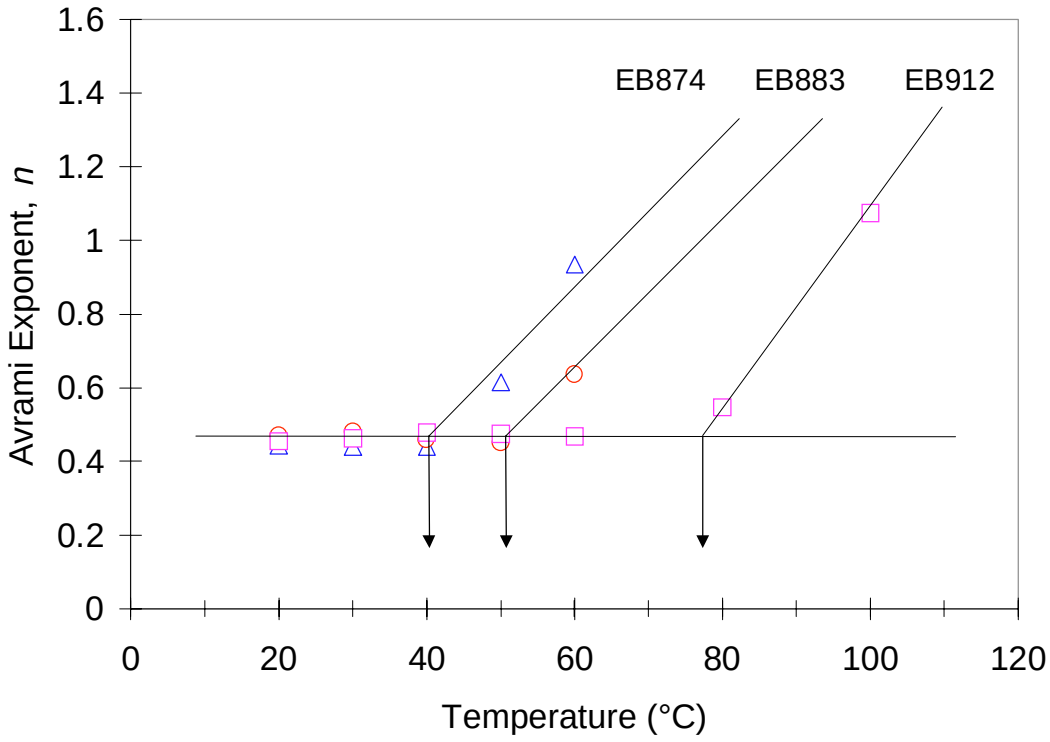

Figure 24 Avrami exponents, *n*, as a function of crystallization temperature for the ethylene/1-butene copolymers of various branch contents

5.7 Discussion

An overview of the results presented above provides a wealth of information regarding the crystallization and melting behaviors of the ethylene/α-olefin copolymers. These results also permit a comparison of these materials to linear polyethylene (LPE), thereby enabling a prediction of the influence of the presence of comonomers on the properties of the copolymers. This section presents a detailed discussion of the observations made above, culminating in the proposal of a qualitative model for the crystallization process in such copolymers. The "universality" of the model for extension to a number of other polymer systems is also discussed.

5.7.1 Comonomer Exclusion

The temporal evolution of the low endotherms in the three types of copolymers follow a similar trend, in spite of significant differences in their side group lengths. In other words, the generation of crystals associated with the low endotherm is not influenced by the branch type present in the copolymer, namely ethyl, propyl or butyl branches. It can then be inferred that these branches are excluded from the crystal lattice, since otherwise the differences in branch length would markedly affect the nature of the crystals. Therefore the branches must be present in the amorphous regions outside of the crystals. Then, as a first approximation, it is possible to use Flory's theory on copolymer crystallization,[11,12,13,14] which was developed for materials in which the comonomers are assumed to be rejected from the crystals. This observation has also been experimentally verified by several investigators.[15,16,17] Mandelkern *et al.*[1] have reported that the melting behavior of ethylene/α-olefin copolymers as a function of their composition is independent of the chemical nature of the branches. Alamo and Mandelkern[2] have made similar observations from infrared and thermal analysis studies on ethylene copolymers.

5.7.2 Dual Crystallization Mechanism

Starting with an examination of the heat capacity curves shown in Figure 3 for EB-912, it is clear that two exothermic processes are involved in the crystallization process from the melt to -20°C. A sharp, high temperature exotherm whose position as well as magnitude are affected by the cooling rate, and a much broader low temperature exotherm extending to temperatures as low as -20°C are observed. On further comparison between copolymers of different branch contents, it is found that both of these exotherms are also influenced by comonomer content. The high temperature exotherm decreases in magnitude and shifts to lower temperatures, whereas the low temperature one increases in magnitude, with increasing comonomer content. These observations are further verified by comparing the crystallinity vs. temperature plots shown in Figure 5 for the ethylene/1-butene copolymers. Two distinct regions of cooling rate variation of $\chi_c(T)$ are observed, corresponding to the two exothermic processes. It is noted that the high temperature exotherm exhibits a strong dependence on cooling rate, while the low temperature one remains largely invariant with the rate of cooling from the melt. The temperature at which the cross-over from cooling rate dependence to cooling rate-independence occurs is referred to as T*, and it is found to be strongly influenced by the comonomer content in the copolymer, as shown in Figure 25. For all three types of copolymers studied, T* is found to shift to higher temperatures with decreasing comonomer content. This is depicted in Figure 25 for the ethylene/1-butene copolymers of varying comonomer contents. Furthermore, it is also noted that T* exhibits an inverse dependence on the cooling rates employed. As mentioned earlier, T* also corresponds to the temperature at which (additional) crystallinity first develops during cooling, and is thereby also referred to as the temperature of incipient crystallization.

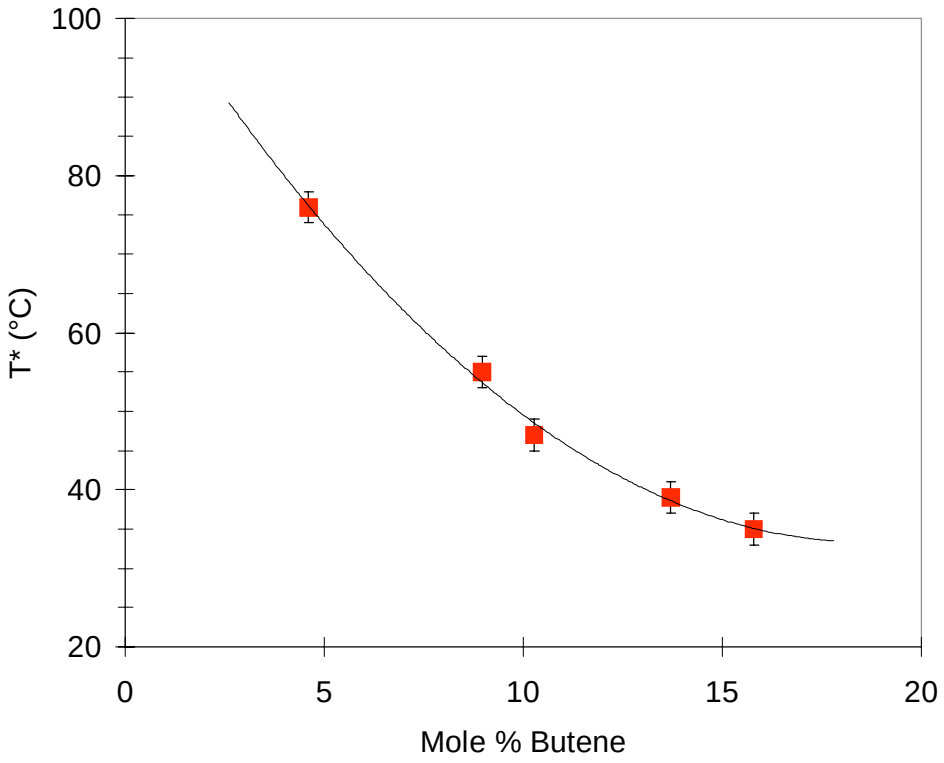

Figure 25 Variation of the cross-over temperature, T*, with comonomer content for the ethylene/1-butene copolymers

Additional evidence for the dual crystallization mechanism may be obtained from the melting traces obtained immediately after cooling from the melt to -20°C, shown in Figure 8 for EB-894 (the crystallinities estimated during cooling to -20°C are also plotted in the figure). Once again, two distinct regions of crystallinity variation with temperature are observed - a low temperature reversible region where the crystallinity values during the heating and cooling cycles are exactly identical to each other, and a high temperature region exhibiting a significant degree of hysteresis between the two sets of data. These two regions correspond to the low and high temperature exothermic processes discussed in the earlier paragraphs respectively. The temperature delineating the hysteretic and reversible regions is identical to the cross-over temperature, T*, alluded to in the previous paragraph.

Further support for the dual crystallization mechanism in the copolymers is derived from the results of the isothermal crystallization experiments carried out above and below T*. The melting traces obtained (below T*) clearly reveal the presence of two melting peaks - a high temperature main melting endotherm and a "low" endotherm (Figure 9). The high melting endotherm corresponds to the melting of crystals formed during cooling from the melt to T_x. Both the position and magnitude of this endotherm remain invariant with crystallization time. The low endotherm is found to evolve ~ 5 to 20°C above the crystallization temperature (T_x). This peak increases in magnitude and shifts to higher temperatures at longer crystallization times (t_x). The position and magnitude of the low endotherm were obtained by means of a deconvolution process described earlier. It is found that for all the copolymers examined, the slopes, B (related to the temporal evolution of the low endotherm position) remain independent of temperature until the temperature T* is reached (Its value is close to 3). Beyond T* the values of B decrease significantly with increasing T_x (Figure 23). A similar transition at T* is observed for the exponents, *n*, derived from the Avrami-type analysis of the low endotherm enthalpies. Below T*, *n* remains independent of temperature with a value close to 0.5, whereas at $T_x > T^*$, its values increase considerably with T_x (Figure 24). Therefore, it is clearly seen that two distinctly different crystallization mechanisms operate in these two temperature regions in these copolymers, and that the temperature T*, marks the cross-over from one to the other.

5.7.3 Cooling Rate-Dependent Hysteretic Region

At this point, it is useful to compare the crystallization behavior of the copolymers to that of linear polyethylene (LPE). The first step in such a comparison is to contrast the trends in the variation of crystallinity as a function of cooling rate, shown in Figure 4 through Figure 7. The copolymers exhibit a clear transition from a cooling rate independent region at lower temperatures to a cooling rate dependent region at the higher temperatures. The crystallinities of LPE, on the other hand display a continuous variation with cooling rates over the entire temperature range studied. It was also mentioned in Section 5.4 that significant hysteresis between the heating and cooling cycles was observed in the case of LPE.[21]

A sizable section of Chapter 2 was dedicated to understanding the predictions made in the polymer crystallization theories and the origin of the experimentally observed deviations from those predictions. It was established that polymer crystallization is governed by kinetic factors more than by thermodynamic ones. This fact is directly responsible for the much lower values for the experimentally observed degrees of crystallinity compared to the equilibrium predictions. It also explains the observation that a finite undercooling is required for the crystallization of polymers at a reasonable rate. The magnitude of the undercooling plays a predominant role in determining the lamellar thickness and morphology of a homopolymer. It can be inferred from the L-H theory for polymer crystallization that the initial crystal thickness should be inversely proportional to the degree of undercooling, at least at low undercoolings. Therefore, the crystallization of a polymer at higher temperatures (closer to the equilibrium melting temperature) yields thicker crystals with higher melting temperatures. This is the case when a polymer is slowly cooled from its melt. However, faster cooling rates correspond to crystallization at lower temperatures, resulting in thinner lamellae with correspondingly lower melting temperatures. These effects explain the cooling rate variation of χ_c over the entire temperature range, for LPE. Furthermore, it has been demonstrated that lamellar crystals melt at temperatures much higher than the temperatures at which they were generated, directly resulting in significant hysteresis between the heating and cooling cycles[50] (as observed for LPE). Then, it may be

concluded that the cooling rate dependence and the hysteresis between the heating and cooling cycles are characteristic of a nucleation controlled chain-folded lamellar growth process.[51,52] The high temperature exothermic process observed for the copolymers displays both of the above features, and can therefore be assigned to such a nucleation controlled growth process leading to the formation of chain-folded lamellae. This assignment is further supported by the observation that the increase in χ_c (on cooling) in the high temperature region is much larger for the lower branched (or more linear-like) copolymers, whose chains have a greater possibility of crystallizing as chain-folded lamellae.

5.7.4 Cooling Rate-Independent Reversible Region

Based on the above discussion, it is clear that the low temperature, *cooling rate-independent, reversible* region is not associated with a lamellar morphology. The following observations are made regarding the nature of crystals formed in this region during the crystallization of copolymers. A gradual increase in χ_c with decreasing temperatures is observed in the copolymer crystallinity curves, even at temperatures as low as -20°C (Figure 5, Figure 6 and Figure 7). [The relative increase in $\chi_c(T)$ in the low temperature region systematically increases with increasing comonomer content]. This is in contrast to the practical invariance of $\chi_c(T)$ at temperatures below ~ 70°C in the corresponding curves for LPE (Figure 4). The low temperature constancy of χ_c for LPE is a reflection of the thickness of the chain-folded lamellar crystals. As alluded to in the previous paragraph, these crystals only melt at temperatures much higher than their crystallization temperatures (T_x). However, the crystals associated with the low endotherm melt at temperatures very close to their crystallization temperatures, especially at short crystallization times. Further confirmation of this fact is derived from the intercepts of the lines in Figure 12**,** Figure 13**,** Figure 14 and Figure 15 (relative positions of the low endotherms as a function of crystallization time at 20°C). As pointed out in the Results section, the melting temperature of the low endotherms (at $T_x < T^*$) consistently extrapolates to the crystallization temperature, for very short crystallization

times. The above result combined with the observed reversibility of copolymer crystallinities (between the heating and cooling cycles) in the low temperature region, implies that the crystals formed are much thinner and possess smaller lateral dimensions than the chain-folded lamellar crystals associated with the high temperature region. Then, it is clear that the cooling rate-independent, reversible region is associated with crystals, whose thicknesses and lateral dimensions are much smaller than those of chain-folded lamellar crystals.

5.7.5 Proposed Mechanism of Copolymer Crystallization

It was established in Chapter 2 that the crystallization process in copolymers is predominantly governed by the crystallizable sequence length distribution, and not the degree of undercooling (as in homopolymers). This fact is directly related to the requirement in Flory's copolymer crystallization theory that only sequences of length greater than a critical length, ζ^*, are allowed to participate in crystal formation. ζ^* increases with increasing T_x, thereby reducing the number of sequences that can form chain-folded crystals. In a random copolymer (such as those used in the present study), the frequent occurrence of branches along the polymer backbone fragments the chain into a number of shorter sequences. At a given crystallization temperature (T_x), some of these sequences may be longer than $\zeta^*(T_x)$ for the copolymer and can form chain-folded lamellar crystals. Further cooling lowers the critical length, allowing shorter sequences to participate in crystal formation. However, the number of such sequences that can result in chain-folded lamellae of reasonable lateral dimensions and perfection decreases with increasing comonomer content. It is also known that the steric stresses built up at the basal planes of the crystals hamper the lateral growth of the lamellae formed by chain-folding. According to the Gambler's Ruin model,[53] these stresses may be minimized by a high degree of adjacent re-entry folding in the lamellae. However, the frequent occurrence of branches along the copolymer backbone hinders such tight folding in the copolymer crystals.

While the longest sequences form part of the lamellar crystals, they impose a considerable degree of constraint on the remaining crystallizable sequences in these chains. As the number of segments participating in lamellar formation increases, so do the restrictions imposed on the mobility of the remaining sequences. At very high degrees of constraint, the shorter sequences are unable to participate in the reeling-in process required for chain-folded crystal formation. The easiest route available for these short segments to crystallize without violating spatial requirements is to simply aggregate into thin bundles with minimum order.[54,55] Accordingly, they aggregate with neighboring sequences to form stable clusters or bundled crystals. These crystals may be visualized as being similar to the fringed-micelles that are considered as the standard morphological form in poorly crystallizable polymers such as poly(vinylchloride). The lateral dimensions of the bundled crystals are restricted by the reduced chain mobility and by the stresses built up at the crystal-amorphous interface. As a result, the bundled crystals melt at temperatures right above their T_x (resulting in the reversibility between $\chi_c(T)$ from cooling and heating), unlike the chain-folded lamellar crystals.

It is also suggested that the bundled crystals may act as cross-linking points in the amorphous phase. When a significant proportion of such crystals are present, they decrease the entropy of the amorphous phase to a considerable extent, thereby causing a shift in the relaxation spectrum of this phase to higher temperatures. This concept may be further verified by following the shift in the relaxation spectrum of the copolymers via mechanical or dielectric experiments. Such verification could provide a correlation between the secondary crystallization process and the time dependence of the mechanical properties of the samples above their glass transition temperatures.

Thus, according to the model for copolymer crystallization proposed above, two distinct modes of crystallization yielding two vastly different morphologies operate in the copolymers. These include the chain-folded lamellar formation from the longest sequences (at higher crystallization temperatures (T_x)) and aggregation of the shorter sequences to form bundled crystals (at lower T_x). A gradual transition from the former to the latter occurs with decreasing T_x and/or increasing comonomer content.

5.7.6 General Observations Based on the Model

The high melting endotherms in the heating traces of a copolymer (subsequent to isothermal crystallization at T_x) (Figure 9) are attributed to the melting of primary chain-folded lamellar crystals formed on cooling from the melt to T_x. The practical invariance in the magnitude of this peak with t_x implies that the primary crystallization is complete even before the start of the isothermal treatment. The low endotherm is associated with the melting of bundled crystals (secondary crystallization) formed by the shorter sequences that were excluded from the primary crystallization.[34,56,57] This idea of a dual crystallization mechanism leading to a dual morphology is consistent with previous studies on ethylene copolymers. Minick *et al.*[18] have reported the existence of lamellae as well as "fringed-micelles" in ethylene/α-olefin copolymers synthesized using the constrained geometry catalyst technology. They observed that copolymers of density between 0.88 and 0.91 g/ml displayed both morphological forms. However, copolymers with density < 0.88 g/ml showed only the "fringed micellar" morphology, while those with densities > 0.91 g/cc only existed as lamellae. Deblieck *et al.*[23] have observed the co-existence of lamellae and nodular entities in ethylene copolymers of varying branch contents. Mathot *et al.*[4] report that the predominant morphology in ethylene/1-octene copolymers varies from the lamellar form at 11% 1-octene content, to a granular structure when the comonomer content is increased to 18%. Darras and Seguela[58,59,60] have reported, based on surface free energy calculations of ethylene/1-butene copolymers, that considerable hindrance to chain folding exists in the highly branched samples. They suggest the presence of random chain folded structures or even "fringed-micelle macroconformations", instead of the lamellar morphology.

It may be inferred from the model that the formation of the low endotherm occurs less readily at low branch concentrations and at higher crystallization temperatures. This prediction is verified by the observation that an ethylene/1-butene copolymer with < 4 mole % 1-butene does not exhibit an observable low endotherm within the experimental time frame. Furthermore, a significant induction time equal to 100 min. is required to detect the presence of an endotherm at (or slightly above) T_x = 60°C, while the process is instantaneous at 20°C for EB-874 (~15 mole % butene). This is due to the fact that

crystallization of the copolymer at 60°C occurs from a completely molten material and is nucleation controlled. As a result, it must be viewed as the primary crystallization process, which explains the considerable induction time involved.

The crystallization model proposed in the previous section can also be applied to describe the variation of the crystallization rate constant, *k*, as a function of comonomer content. The shape of the curve obtained (Figure 17) is explained by the availability of crystallizable chain segments at a given temperature. For LPE (devoid of branches) most of the chains crystallize during cooling via the lamellar growth process. The number and mobility of crystallizable sequences in the remaining amorphous fraction is severely limited by the relatively regular chain-folding process. For a highly branched copolymer, the number of sequences long enough to form crystals is considerably reduced. Therefore, the value of *k* for both these cases approaches zero, and a maximum in the *k* vs. comonomer content curve is observed for an intermediate branch content copolymer.

The value of 0.5 obtained for the Avrami exponent, *n*, at $T_x < T^*$ has been interpreted in more than one way, including that of a diffusion controlled one-dimensional growth.[47] It may also be possible to explain this value based on a fractal-type growth process.[4] The increase in *n* and decrease in B at $T_x > T^*$ (higher temperatures) is consistent with increasingly amenable conditions for a chain-folded process. The values of *n* at higher temperatures may be visualized as approaching those of LPE (*n* = 3 to 4), which is predominantly constituted of chain-folded lamellae.

5.7.7 Long-Time Dependence of the Low Endotherm

The temporal evolution of the low endotherms formed during the isothermal crystallization of the ethylene/α-olefin copolymers at different T_x's have been studied in detail. The enthalpies associated with the endotherms increase only very slowly at long crystallization times ($t_x > 10^2 - 10^3$ min). However, the relative position of the low endotherm continues to shift to higher temperatures even beyond those long crystallization times.

Several interpretations have been provided for the shifting of the melting endotherm to higher temperatures at longer t_x. A common one associated with flexible polymers such as LPE is the lamellar thickening mechanism.[56,57,47] It was mentioned in Chapter 2 that this process is thermodynamically favorable since it reduces the specific surface of polymer crystals. However, this mechanism requires a fair degree of chain mobility and a means of chain transport from the amorphous to the crystalline layers. As a result, it is expected to occur only in polymers that exhibit the crystal α-relaxation. In the case of the ethylene/α-olefin copolymers used in the present study, the branches that are excluded from the crystals accumulate at the crystal-amorphous interface, thereby preventing the thickening of lamellae. A similar explanation can be extended to the bundled crystals associated with the low endotherm. Their thickness along the *c*-axis is severely restricted by the relatively short crystallizable sequence lengths. The lateral dimensions of these crystals are limited by the stresses built up at the crystal surface (due to the differences in packing density between the crystalline and adjoining amorphous regions. Such variations could be related to the accumulation of branches and to the lack of sufficient adjacent re-entry chain folding). Therefore, lamellar thickening can be ruled out as a possible explanation for the long time dependence of the low endotherm positions. An increase in crystal perfection of the bundled crystals is also not very likely for the same reasons.

It is suggested, based on the crystallization model proposed earlier, that the shifting of the low endotherm positions to higher temperatures with longer crystallization times is due the decreasing conformational entropy of the remaining amorphous fraction in the copolymer. This idea is consistent with the concept of the bundled crystals acting as cross-links in the amorphous phase. Then, it can be seen how the degree of constraint in the amorphous phase increases with an increasing fraction of such crystals, causing the relaxation spectrum of the amorphous phase to shift to higher temperatures as well. Direct correlations between the rate of temporal evolution of the low endotherm and that of the glass transition temperature have been made on the following polymers investigated in our laboratory - PEEK[25,61], PET[26] and *i*-PS[61]. It has also been demonstrated in a recent publication from our laboratory[21] that the upward shift of the low endotherm is associated with an increase in the melt free energy rather than with a

lowering of the crystal free energy. The increase in melt free energy is associated with the decreasing entropy of the remaining amorphous fraction during the formation of bundled crystals.

In this chapter, the results from the thermal analysis experiments on the copolymers were examined in detail. Two distinct crystallization mechanisms leading to vastly different crystal morphologies were observed. In the next chapter, the morphologies discussed in this chapter are examined via Atomic Force Microscopy (AFM).

[1] R. Alamo, R. Domszy and L. Mandelkern, *J. Polym. Phys.*, **88**, 6587 (1984)
[2] R. G. Alamo, L. Mandelkern, *Macromolecules*, **22**, 1273 (1989)
[3] S. D. Clas, D. C. McFaddin, K. E. Russell, M. V. Scannell-Bullock and I. R. Peat, *J. Polym. Sci. Polym. Chem. Ed.*, **25**, 3105 (1987)
[4] V. B. F. Mathot, R. L. Scherrenberg and T. F. J. Pijpers, *Polymer*, **39**, 4541 (1998)
[5] V. B. F. Mathot and M. F. Pijpers, *J. Appl. Polym. Sci.*, **39**, 979 (1990)
[6] T. Krigas, J. Carella, M. Strugklinski, B. Crist, W. W. Graessley and F. C. Schilling, *J. Polym. Sci. Polym. Phys. Ed.*, **23**, 509 (1985)
[7] B. Crist and P. R. Howard, *Macromolecules*, **32**, 3057 (1999)
[8] C. J. Stacy and R. L. Arnett, *J. Phys. Chem.*, **77**, 78 (1973)
[9] H. Rachapudy, G. G. Smith, V. R. Raju and W. W. Graessley, *J. Polym. Sci. Polym. Phys. Ed.*, **17**, 1211 (1979)
[10] W. E. Rochefort, G. G. Smith, H. Rachapudy, V. R. Raju and W. W. Graessley, *J. Polym. Sci. Polym. Phys. Ed.*, **17**, 1197 (1979)
[11] P. J. Flory, *J. Chem. Phys.*, **17**, 3, 223 (1949)
[12] P. J. Flory, *Trans. Faraday Soc.*, **51**, 848 (1955)
[13] R. Chiang and P. J. Flory, *J. Am. Chem. Soc.*, **83**, 2857 (1961)
[14] P. J. Flory, "*Principles of Polymer Chemistry*", Cornell University Press, Ithaca, N.Y., 1953
[15] C. H. Baker and L. Mandelkern, *Polymer*, **7**, 7 (1966)
[16] M. J. Richardson, P. J. Flory and J. B. Jackson, *Polymer*, **4**, 221 (1963)
[17] E. Perez, D. L. VanderHart, B. Crist and P. R. Howard, *Macromolecules*, **20**, 78 (1987)
[18] J. Minick, A. Moet, A. Hiltner, E. Baer and S. P. Chum, *J. Appl. Polym. Sci.*, **58**, 1371 (1995)
[19] M. Peeters, B. Goderis, C. Vonk, H. Reynaers and V. Mathot, *J. Polym. Sci. Polym. Phys. Ed.*, **35**, 2689 (1997)
[20] B. Wunderlich, *The Athas Data Base on Heat Capacities of Polymers, Pure and Applied Chem.*, **67**, 1919 (1995)
[21] A. Alizadeh, L. Richardson, J. Xu, S. McCartney and H. Marand, *Submitted to Macromolecules*
[22] L. Mandelkern, M. Glotin and R. A. Benson, *Macromolecules*, **14**, 22 (1981)
[23] R. A. C. Deblieck and V. B. F. Mathot, *J. Mater. Sci. Let.*, **7**, 1276 (1988)
[24] F. Sakaguchi, L. Mandelkern and J. Maxfield, *J. Polym. Sci. Polym. Phys. Ed.*, **14**, 2137 (1976)
[25] H. Marand, A. Alizadeh, R. Desai, R. Farmer, V. Velikov and V. Prabhu, *Bull. Am. Phys. Soc.* (1999)
[26] H. Marand, P. Sholtz, R. Verma, V. Prabhu and J. Vivirito, *Bull. Am. Phys. Soc.*, **41(1)**, 450 (1996)
[27] S. Sohn, A. Alizadeh and H. Marand, *Bull. Am. Phys. Soc.* (1999)
[28] A. Alizadeh, J. Quinn, S. Sohn, L. Richardson and H. Marand, *Bull. Am. Phys. Soc.* (1999)
[29] M. Avrami, *J. Chem. Phys.*, **7**, 1103 (1939)
[30] M. Avrami, *J. Chem. Phys.*, **8**, 212 (1940)
[31] M. Avrami, *J. Chem. Phys.*, **9**, 177 (1941)
[32] P. C. Hiemenz, "*Polymer Chemistry: The Basic concepts*", Marcel Dekker Inc., New York, Chapter 4 (1984)
[33] B. Wunderlich, "*Macromolecular Physics*", Vol. 2, Academic Press, New York (1976)
[34] J. Schultz, "*Polymer Materials Science*", Prentice-Hall Inc., Englewood Cliffs, New Jersey (1974)
[35] V. F. Goler and G. Sachs, *Z. Phys.*, **77**, 281 (1932)
[36] R. G. Alamo and L. Mandelkern, *Macromolecules*, **24**, 6480 (1991)
[37] L. Mandelkern, "*Crystallization of Polymers*", McGraw Hill, New York, p. 215 (1964)
[38] L. Mandelkern, F. A. Quinn Jr. and P. J. Flory, *J. Appl. Phys.*, **12**, 97 (1954)
[39] F. Rybnikar, *J. Polym. Sci.*, **44**, 517 (1960)
[40] E. W. Fischer, *Pure Appl. Chem.*, **31(1)**, 113 (1972)
[41] E. W. Fischer and G. F. Schmidt, *Angew. Chem. (Intern. Ed. Engl.)*, **1**, 488 (1962)
[42] D. T. Grubb, J. H. Liu, M. Caffrey and D. H. Bilderback, *J. Polym. Sci. Polym. Phys. Ed.*, **22**, 367 (1984)
[43] J. H. Magill, in "*Treatise on Materials Science and Technology: Properties of Solid Polymeric Materials*": Part A, Ed., J. M. Schultz, Vol. 10, Academic Press, New York (1977)

[44] J. P. Runt in "*Encyclopedia of Polymer Science and Engineering*", Ed., J. I. Kroschwitz, Wiley, New York, 2nd Edition, Vol. 4, 482 (1990)
[45] G. M. Stack, L. Mandelkern and I. G. Voigt-Martin, *Polym. Bull.*, **8**, 421 (1982)
[46] A. Booth and J. H. Hay, *Polymer*, **10**, 95 (1969)
[47] J. M. Schultz and R. D. Scott, *J. Polym. Sci. A-2*, **7**, 659 (1969)
[48] H. D. Keith, F. J. Padden, Jr. and R. G. Vadimsky, *J. Appl. Phys.*, **42**, 4585 (1971)
[49] D. W. van Krevelen, *Chimia*, **32**, 279 (1978)
[50] J. D. Hoffman, G. T. Davis, J. I. Lauritzen, Jr., *Treatise on Solid State Chemistry*, Ed. N.B. Hannay, Plenum Press, N.Y., Vol. 3, Chap. 7 (1976)
[51] J. D. Hoffman, L. J. Frolen, G. S. Ross and J. I. Lauritzen Jr., *J. Res. Natl. Bur. Stand., Sect. A*, **79**, 671 (1975)
[52] J. Maxfield and L. Mandelkern, *Macromolecules*, **10**, 1141 (1977)
[53] C. M. Guttman, E. DiMarzio and J. D. Hoffman, *Polymer*, **22**, 1466 (1981)
[54] P. J. Flory and A. D. McIntyre, *J. Polym. Sci.*, **18**, 592 (1955)
[55] M. Takayanagi and T. Yamashita, *J. Polym. Sci.*, **22**, 552 (1956)
[56] J. D. Hoffman and J. J. Weeks, *J. Chem. Phys.*, **42**, 4301 (1965)
[57] B. Wunderlich and J. Mellilo, *Macromol. Chem.*, **118**, 250 (1968)
[58] R. Seguela and F. Rietsch, *Polymer*, **27**, 703 (1986)
[59] R. Seguela and F. Rietsch, *J. Mat. Sci.*, **23**, 415 (1988)
[60] O. Darras and R. Seguela, *Polymer*, **34**, 2946 (1993)
[61] V. Velikov, *Ph.D Dissertation*, Virginia Polytechnic Institute & State University (1996)